The synapsin-dependent vesicle cluster is crucial for presynaptic plasticity at a glutamatergic synapse in male mice

Felicitas Bruentgens[1,2], Laura Moreno Velasquez[1,2,*], Alexander Stumpf[1,2,*], Daniel Parthier[1,2,3], Jörg Breustedt[1,2], Fabio Benfenati[4,5], Dragomir Milovanovic[1,6,7], Dietmar Schmitz[1,2,3,6,7,8,§], Marta Orlando[1,2,§]

1 Charite´ – Universitätsmedizin Berlin, corporate member of Freie Universität Berlin and Humboldt-Universität zu Berlin, Charitéplatz 1, 10117 Berlin, Germany, **2** Charite´ – Universitätsmedizin Berlin, corporate member of Freie Universität Berlin and Humboldt-Universität zu Berlin, NeuroCure Cluster of Excellence, 10117 Berlin, Germany, **3** Max Delbrück Center for Molecular Medicine in the Helmholtz Association, Robert-Rössle-Straße 10, 13125 Berlin, Germany, **4** Center for Synaptic Neuroscience and Technology, Istituto Italiano di Tecnologia, 16163 Genoa, Italy, **5** IRCCS Ospedale Policlinico San Martino, 16132 Genoa, Italy **6** German Center for Neurodegenerative Diseases (DZNE) Berlin, 10117 Berlin, Germany, **7** Charite´ – Universitätsmedizin Berlin, corporate member of Freie Universität Berlin and Humboldt-Universität Berlin, Einstein Center for Neurosciences, 10117 Berlin, Germany, **8** Humboldt-Universität zu Berlin, Bernstein Center for Computational Neuroscience, Philippstraße 13, 10115 Berlin, Germany

***** These authors contributed equally

§ Corresponding authors, e-mail addresses: marta.orlando@charite.de, dietmar.schmitz@charite.de

Conflict of interest statement:

The authors have declared that no competing interests exist.

Acknowledgements

This study was supported by the Deutsche Forschungsgemeinschaft (DFG, German Research Foundation), project 184695641 – SFB 958 (to D.S.), project 327654276 – SFB 1315 (to D.S.), project 415914819 – FOR 3004 (to D.S.), project 431572356 (to D.S.), under Germany's Excellence Strategy EXC-2049-390688087 (NeuroCure; to D.S. and M.O), project 503954250 (to M.O.). It was also supported by the European Research Council (ERC) under the European Union's Horizon 2020 research and innovation program (BrainPlay Grant agreement No. 810580; to D.S.) and by the Federal Ministry of Education and Research (BMBF, SmartAge – project 01GQ1420B; to D.S.). D.M. is supported by

the start-up funds from DZNE, the grants from the German Research Foundation (SFB 1286/B10 and MI 2104), and the Human Frontiers Science Organization (RGEC32/2023). The funders had no role in study design, data collection and analysis, decision to publish, or preparation of the manuscript.

We thank Susanne Rieckmann for excellent technical assistance. We thank Anke Schönherr and Caterina Michetti for organizational matters with SynTKO animals; as well as Christian Hoffmann and Franziska Trnka for assistance in obtaining the necessary animal permits for the SynTKO line. We thank the Electron Microscopy Laboratory of the Institute of Integrative Neuroanatomy and the Core Facility for Electron Microscopy of the Charité for granting us access to their instruments. Finally, we thank Antje Fortströer for careful revision of our manuscript.

Data availability statement

Data is fully available on request. Moreover, we are curating it for uploading it to zenodo.

Author contributions

Conceptualization: Marta Orlando, Dietmar Schmitz

Methodology: Alexander Stumpf, Laura Moreno Velasquez, Jörg Breustedt, Marta Orlando

Software: Daniel Parthier

Validation: Felicitas Bruentgens, Laura Moreno Velasquez, Alexander Stumpf, Daniel Parthier, Jörg Breustedt, Dietmar Schmitz, Marta Orlando

Formal analysis: Felicitas Bruentgens, Laura Moreno Velasquez, Alexander Stumpf, Daniel Parthier

Investigation: Felicitas Bruentgens, Laura Moreno-Velasquez, Alexander Stumpf, Marta Orlando

Resources: Fabio Benfenati, Dragomir Milovanovic, Dietmar Schmitz

Data Curation: Felicitas Bruentgens, Marta Orlando

Writing – Original Draft: Felicitas Bruentgens, Marta Orlando

Writing – Review and Editing: Felicitas Bruentgens, all co-authors.

Visualization: Felicitas Bruentgens

Supervision: Marta Orlando, Jörg Breustedt, Dietmar Schmitz

Project administration: Felicitas Bruentgens, Marta Orlando, Laura Moreno Velasquez

Funding acquisition: Dietmar Schmitz, Marta Orlando

Abbreviations

SynI, synapsin I; SynII, synapsin II; SynIII, synapsin III; KO, knockout; SynDKO, synapsin double knockout; SynTKO, synapsin triple knockout; LTP, long-term potentiation; STP, short-term plasticity; RRP, readily releasable pool; PPR, paired-pulse ratio; PTP, post-tetanic potentiation; WT, wildtype; fEPSP, excitatory postsynaptic field potential; SEM, standard error of the mean; TEM, transmission electron microscopy; PKA, protein-kinase A; ACSF, artificial cerebrospinal fluid; S-ACSF, sucrose-artificial cerebrospinal fluid; DCG-IV, (2S,1'R,2'R,3'R)-2-(2,3-dicarboxycyclopropyl)glycine; RRID, research resource identifier; WT, wildtype

ABSTRACT

Synapsins are highly abundant presynaptic proteins that play a crucial role in neurotransmission and plasticity via the clustering of synaptic vesicles. The synapsin III isoform is usually downregulated after development, but in hippocampal mossy fiber *boutons* it persists in adulthood. Mossy fiber *boutons* express presynaptic forms of short- and long-term plasticity, which are thought to underlie different forms of learning. Previous research on synapsins at this synapse focused on synapsin isoforms I and II. Thus, a complete picture regarding the role of synapsins in mossy fiber plasticity is still missing. Here, we investigated presynaptic plasticity at hippocampal mossy fiber *boutons* by combining electrophysiological field recordings and transmission electron microscopy in a mouse model lacking all synapsin isoforms. We found decreased short-term plasticity - i.e. decreased facilitation and post-tetanic potentiation - but increased long-term potentiation in male synapsin triple knockout mice. At the ultrastructural level, we observed more dispersed vesicles and a higher density of active zones in mossy fiber *boutons* from knockout animals. Our results indicate that all synapsin isoforms, including synapsin III, are required for fine regulation of short- and long-term presynaptic plasticity at the mossy fiber synapse.

Significance statement

Synapsins cluster vesicles at presynaptic terminals and shape presynaptic plasticity at giant hippocampal mossy fiber *boutons*. Deletion of all synapsin isoforms results in decreased short- but increased long-term plasticity.

Introduction

Neurotransmission is a fundamental process that enables us to sense the world around us, to react to it, to think, learn and remember. This process requires high temporal and spatial fidelity, and the energy-expensive and complex regulation of synaptic vesicle trafficking is a prerequisite. A crucial aspect is the spatial arrangement of neurotransmitter-filled vesicles inside the synapse, regulated by the protein family of synapsins (Atias et al., 2019; Sansevrino et al., 2023).

Synapsins are highly abundant phosphoproteins associated with the surface of synaptic vesicles (De Camilli et al., 1990; Cesca et al., 2010), encoded by three mammalian genes (*SYN1, SYN2, SYN3*) (Südhof et al., 1989; Kao et al., 1998). Impairment of synapsin I (SynI) and II (SynII) causes vesicle dispersion and shrinks the distal vesicle cluster, the reserve pool (Li et al., 1995; Pieribone et al., 1995; Rosahl et al., 1995). Thus, synapsins main function is to control mobilization from the reserve pool, in a phosphorylation-dependent manner (Sihra et al., 1989; Hosaka et al., 1999; Chi et al., 2001). How synapsins preserve this pool is still under debate. Likely mechanisms are: (1) synapsins crosslink the vesicles, acting as tethers (Hirokawa et al., 1989), (2) synapsins form a liquid phase, capturing vesicles in it (Milovanovic et al., 2018; Pechstein et al., 2020) or (3) a mixture of both, since these mechanisms are not mutually exclusive (Zhang and Augustine, 2021; Song and Augustine, 2023).

While SynI and SynII are expressed in mature synapses (De Camilli et al., 1983; Browning et al., 1987), synapsin III (SynIII) is primarily expressed during development: after one week postnatal its levels decrease drastically (Ferreira et al., 2000) and remain low in adults (Kao et al., 1998). However, in brain regions featuring postnatal neurogenesis, SynIII is still expressed in adult tissue (Pieribone et al., 2002). This includes the dentate gyrus and hippocampal mossy fibers.

Hippocampal mossy fibers are thought to be involved in learning, memory and spatial navigation (Rolls, 2018). They connect granule cells and CA3 pyramidal cells via mossy fiber *boutons*, highly-plastic synapses (Nicoll and Schmitz, 2005). Activity-dependent changes in neurotransmission can be studied very well in these *boutons*, because they can react to a wide range of frequencies (Salin et al., 1996) and express presynaptic short- and long-term potentiation (STP, LTP) (Zalutsky and Nicoll, 1990; Nicoll and Schmitz, 2005). Recently, a mechanism for short-term memory has been proposed: the formation of a "pool engram" – an increased readily releasable pool (RRP) – which could depend on the vesicle mobilization via synapsins (Vandael et al., 2020). Unlike STP, mossy fiber LTP is still more enigmatic: It is known to be protein kinase A (PKA)-dependent (Weisskopf et al., 1994), but the precise downstream targets and potential parallel mechanisms are not yet clarified (Monday et al., 2018, 2022; Shahoha et al., 2022).

Synapsin-dependent mossy fiber physiology has been investigated in SynI/SynII double knockout (SynDKO) animals (Spillane et al., 1995; Owe et al., 2009): field recordings revealed impaired frequency facilitation in physiologically relevant ranges (Owe et al., 2009), while LTP was unchanged (Spillane et al., 1995). However, enrichment of SynIII close to the active zone at mossy fiber *boutons* (Owe et al., 2009) raised the question, if the additional knockout (KO) of SynIII would have further effects on mossy fiber transmission and plasticity.

Here, we examined a glutamatergic synapse that retains SynIII expression in adulthood and asked how neurotransmission is changed upon the complete loss of synapsins. We investigated this question in acute slices of SynI/SynII/SynIII triple knockout (SynTKO) male mice using a combined approach of transmission electron microscopy (TEM) and electrophysiological field recordings. We observed fewer vesicles in the reserve pool and increased active zone density. Field recordings provided evidence that synapsins are crucial for both STP and LTP in mossy fibers: facilitation and post-tetanic potentiation were impaired, while LTP was enhanced.

Methods

Reporting guidelines

This study was reported in accordance with the SAGER guidelines (Heidari et al., 2016) and ARRIVE guidelines 2.0 (Percie du Sert et al., 2020). The checklist for the SAGER guideline is provided in table 1, the checklist for the essential ten of the ARRIVE guideline is provided in table 2 and the checklist for the recommended set of the ARRIVE guideline is provided in table 3.

Ethics statement

All animal experiments were carried out according to the guidelines stated in Directive 2010/63/EU of the European Parliament on the protection of animals used for scientific purposes and were approved by the animal welfare committee of Charité – Universitätsmedizin Berlin and the Landesamt für Gesundheit und Soziales (LaGeSo) Berlin (permit T 0100/03 and permit G 0146/20).

Study design

In this study, only male mice were used for experiments to exclude possible indirect estrogen effects on mossy fiber plasticity (Harte-Hargrove et al., 2013). In electrophysiological recordings, C57BL/6J control mice (RRID:IMSR_JAX:000664) were compared to SynI/SynII/SynIII triple knockout (SynTKO) mice (RRID:MMRRC_041434-JAX) in two age groups: one younger group (4-6 weeks of age), which is referred to as presymptomatic, and one older group (17-19 weeks of age), which is referred to as symptomatic. These terms describe the phenotype before and after the onset of epileptic seizures in SynTKO animals, respectively (Farisello et al., 2013). SynTKO mice were purchased from the Jackson Laboratory (RRID:SCR_004633) and were based on work from Gitler and coworkers (Gitler et al., 2004). The presymptomatic SynTKO data were obtained from two different cohorts. We received the first cohort from Prof. Dr. Fabio Benfenati (Instituto Italiano di Tecnologia, Genova, Italy). The second cohort from Dr. Dragomir Milovanovic (DZNE, Berlin, Germany) was housed and bred in the Charité animal facility (FEM; Forschungseinrichtungen für Experimentelle Medizin). Symptomatic SynTKO animals and all control animals were also bred and born in the Charité animal facility. For each experiment we were aiming for at least three biological replicates (animals) per group. Depending on

163 experimental success (how many recordings needed to be excluded, technical failures), we added more
164 animals per group.

165 Field recordings

166 Data from both presymptomatic SynTKO cohorts were pooled, because they were not significantly
167 different (Table 4). Field recording experiments in all four groups (WT, SynTKO, presymptomatic,
168 symptomatic) were repeated with at least three mice from more than one litter (Table 5). Variable *s*
169 represents the number of recorded slices while *a* reports the number of animals. We were not blinded
170 towards the genotype, because the phenotype was too strong.

171 Recordings were excluded when they had a baseline fEPSP smaller than two times noise (Table 6).
172 Noise was approximately 25 µV, so the baseline fEPSP amplitude needed to be at least 50 µV to be
173 included. Furthermore, to include only mossy fiber specific recordings, we applied 1 µM DCG-IV
174 (#0975, Tocris Bioscience) at the end of each experiment (Kamiya et al., 1996). If the suppression was
175 75% or more, the recording was included (Table 6). We were not able to measure input-output curves
176 for all animals. For those cases where it was not recorded with different input strengths, we took the
177 averaged baseline values for PFV and fEPSP, respectively. If the PFV could not be measured
178 unambiguously, this measurement was excluded from the input-output graph. If the 1 Hz or 25 Hz
179 induction failed, the respective measurements were excluded for analysis, but all other parameters from
180 the same experiment were included. The same was true for some recordings, in which no 25 Hz
181 stimulation and thus no PTP and LTP recordings were conducted. If possible, two mice with different
182 genetic backgrounds were recorded on the same day to minimize variability due to experimental day.

183 Transmission electron microscopy

184 For ultrastructural investigation of mossy fiber *boutons* male mice at the age of 4-6 weeks were used.
185 Data from the two presymptomatic SynTKO cohorts were pooled. For vesicle numbers and mean nearest
186 neighbor distance we identified mossy fiber *boutons* from two young WT and three SynTKO mice. We
187 imaged serial sections from 12 WT and 16 SynTKO mossy fiber *boutons*, respectively. For active zone
188 density we analyzed partial 3D reconstructions of mossy fiber *boutons* from three WT and three
189 SynTKO animals. Slices from each animal were either treated with forskolin or allocated as control.

Allocation of slices to treatment or control group was block-randomized. Replicates of 17 (WT), 16 (WT + forskolin), 16 (SynTKO) and 18 (SynTKO + forskolin) mossy fiber *boutons* were analyzed. Number n represents the number of presynaptic *bouton* reconstructions. The experimenter was blinded to the treatment of slices from fixation of the slices until the end of analysis. Due to the strong reduction in vesicle density of SynTKO synapses, blinding during analysis was only possible between treatment groups, but not between genotypes.

Acute slice preparation

Animals were kept in a 12L:12D hour light-dark cycle and water and food were provided *ad libitum*. Cages offered shelter in form of a house and tubes. Cages of SynTKO animals were kept in remote shelves to minimize exposure to light and possible noises. The first cohort of presymptomatic SynTKO animals was imported from Italy and allowed to sit in the Charité animal facility for several days before the experiments started. After transfer from the animal facility to the preparation room, all animals were allowed to acclimate to the new surrounding for at least half an hour. Acute brain slices were prepared as follows: Mice were anaesthetized under the hood with isoflurane and quickly sacrificed with sharp scissors. The brain was taken out and placed in oxygenated ice-cold sucrose-artificial cerebrospinal fluid (S-ACSF) for three minutes to allow equilibration. S-ACSF contained in mM: 50 NaCl, 25 $NaHCO_3$, 10 Glucose, 150 Sucrose, 2.5 KCl, 1 NaH_2PO_4, 0.5 $CaCl_2$, 7 $MgCl_2$. All solutions were saturated with 95% O_2 (vol/vol) / 5% CO_2 (vol/vol) and had a pH of 7.4 and an osmolarity of 340 mOsm. Hemispheres were separated and 300 µm/150 µm (field recordings/electron microscopy) thick sagittal sections were cut from both hemispheres with a vibratome (VT1200 S, Leica Biosystems (RRID:SCR_018453)). Slices were stored in a submerged chamber in oxygenated S-ACSF at 34°C for half an hour before they were moved to another submerged chamber with artificial cerebrospinal fluid (ACSF) at room temperature. There, slices were kept until the start of experiments. ACSF had an osmolarity of 300 mOsm and a pH of 7.4 and contained the following substances in mM: 119 NaCl, 26 $NaHCO_3$, 10 Glucose, 2.5 KCl, 1 NaH_2PO_4, 2.5 $CaCl_2$, 1.3 $MgCl_2$. All chemicals were purchased from Sigma Aldrich.

Field recordings

Slices were kept in a submerged chamber with ACSF at least 30 minutes and up to six hours before start of recordings. Slices were placed in a recording chamber under a microscope and were continuously superfused with oxygenated ACSF at room temperature at a rate of approximately 2.5 ml/min. The recording electrode was fixed in a headstage of the amplification system (Axon Instruments, MultiClamp 700A/700B (RRID:SCR_018455)). Stimulation and recording electrode units were placed on micromanipulators (Mini 23/25, Luigs & Neumann GmbH) for precise movement control via a control system (SM-5/-7/-10, Luigs & Neumann GmbH).

The stimulation and recording electrodes were prepared from silver wires (AG-8W and E-205, Science Products). Glass pipettes were made from borosilicate capillaries (GB150EFT-10, Science Products or #1403005, Hilgenberg) with a pipette puller (PC-10, Narishige or DMZ-Universal Puller, Zeitz-Instrumente) and were broken at the tip with a micro forge (MF-830, Narishige) to receive low-resistance pipettes. Electrodes were placed in the hilus of the dentate gyrus near the granule cell layer (stimulation) and within the *stratum lucidum* of the area CA3 of the hippocampus (recording), respectively.

Stimulations were executed with a stimulation box (ISO-Flex, A.M.P.I. (RRID:SCR_018945)) and stimulation patterns were controlled with a Master 8 generator (A.M.P.I. (RRID:SCR_018889)). Igor Pro (version 6, WaveMetrics (RRID:SCR_000325)) was used for signal acquisition. The Axon MultiClamp amplifier (700A/700B, Molecular Devices (RRID:SCR_018455)) was used in current clamp mode I=0, with filtering of 2 kHz. Signals were digitized (Axon Digidata 1550B, Molecular Devices / BNC-2090; National Instruments Germany GmbH) at a rate of 20 kHz. Mossy fiber signals were searched by placing the stimulation and recording electrodes at different locations in the hilus and *stratum lucidum*, respectively. Once a mossy fiber input was obtained, the recording was started and the mossy fibers were stimulated at 0.05 Hz.

The standard stimulation frequency was 0.05 Hz throughout the experiment, unless otherwise stated. Recorded sweep length was 0.5 s except for the high-frequency stimulation at 25 Hz where 5.5 s were

recorded. First, input-output relations were recorded by applying different input currents via the stimulation box. The strength of the input current was adjusted to yield a specific presynaptic fiber volley size: 0.05 mV, 0.1 mV, 0.2 mV, 0.3 mV and maximum (maximal stimulation strength of 10 mA). Each input strength was recorded for three sweeps. Afterwards, a medium stimulation strength was chosen and a baseline was recorded for at least ten sweeps. Then, the stimulation frequency was increased to 1 Hz for 20 sweeps for recording of frequency facilitation. Afterwards, when fEPSP amplitudes declined to baseline level again, a paired-pulse with an inter-stimulus interval of 50 ms was applied for three sweeps. Then, a baseline was recorded for 10 minutes (30 sweeps, except for once when only 20 sweeps were recorded) before a high-frequency train of stimuli was given: four times 125 pulses at 25 Hz every 20 seconds with a recorded sweep length of 5.5 seconds. Post-tetanic potentiation and subsequently long-term potentiation were measured for at least 30 minutes after the tetanus. Mossy fiber purity of signals was verified at the end of each recording with the application of 1 µM DCG-IV (#0975, Tocris Bioscience). All recordings with a suppression of at least 75% of the signal were used for analysis.

Field recording analysis

Field recordings were analyzed with Igor Pro (versions 6 and 8, WaveMetrics (RRID:SCR_000325)) and the installed plugin NeuroMatic (RRID:SCR_004186) as well as Microsoft Excel (RRID:SCR_016137). Igor Pro is commercially available at https://www.wavemetrics.com/products/igorpro and Microsoft Excel is commercially available at https://www.microsoft.com/de-de/microsoft-365/excel. Presynaptic fiber volleys (PFV) were measured peak to peak. Field EPSP amplitudes were baseline-corrected and measured +/- 2 ms around the peak. For input-output curves, the mean value of the three sweeps at the same stimulation strength was taken, except for the cases in which no input-output curve was recorded: here, we took the average size of PFV and fEPSP amplitude from the initial baseline. Field EPSP amplitudes during 1 Hz facilitation were normalized to the initial baseline (10 sweeps, 3 minutes). The paired-pulse ratio (PPR) was calculated as the ratio between the second to the first fEPSP amplitude. The stated PPR refers to the first of three paired stimulations. For analysis of the high-frequency trains we normalized the fEPSP amplitudes to the baseline before (30 sweeps, 10 minutes). We also evaluated the PFV size for a subset of fEPSPs of the 25 Hz trains. We measured the PFV for stimuli 10-15 and averaged those six values for the first and

fourth stimulation train, respectively (Figure 2-1b). Also, we calculated the ratio of those averaged values between fourth and first stimulation train, to compare the relative loss of PFV size (Figure 2-1c). Values for PTP and LTP were normalized to the average of the recorded baseline before high-frequency stimulation (30 sweeps, 10 minutes). Values for LTP were the averaged fEPSP amplitudes from minute 20-30 (30 sweeps) after induction. At the end of the recording, specificity was verified by application of DCG-IV. We averaged the last 15 sweeps of DCG-IV wash-in for quantification. Recordings, in which the suppression was less than 75% were not counted as mossy fiber-specific and were not included in the analysis.

Conventional electron microscopy

After preparation, acute slices were allowed to recover in ACSF at room temperature for at least 30 minutes. Subsequently we induced chemical LTP in half of the slices by incubating them in 50 µM forskolin (AG-CN2-0089-M050, Cayman Chemical), solved in DMSO, for 15 minutes at room temperature in oxygenated ACSF (Orlando et al., 2021). The other half of the slices (controls) were incubated in ACSF containing the same concentration of DMSO as the treatment group. Treatment was allocated following a block randomization design. Subsequently, we moved the slices under a chemical hood where fixation, post-fixation, staining, dehydratation, and infiltration steps were performed. We fixed proteins by immersing brain slices in a solution containing 1.25% glutaraldehyde (#E16216, Science Services) in 66 mM NaCacodylate (#E12300, Science Services) buffer for 1 hour at room temperature. After washes in 0.1 M NaCacodylate buffer slices were postfixed in 1% OsO_4 in 0.1 M NaCacodylate buffer for 1 hour at room temperature. Slices were then washed and stained en bloc with 1% uranyl acetate (#1.08473, Merck) in dH_2O and dehydrated in solutions with increasing ethanol concentration (70%, 80%, 96%, 100%). Final dehydration was obtained by incubating slices in propylene oxide (#20401, Electron Microscopy Sciences). The infiltration of epoxy resin was obtained by serial incubations in increasing resin/propylene oxide dilutions (1:3; 1:1; 3:1). Samples were finally flat embedded in Epon (#E14120-DMP, Science Services) for 48 hours at 60°C. The *stratum lucidum* in the CA3 region of the hippocampus was identified in 700 nm semi-thin sections stained with Toluidine blue (Sigma) using a light microscope (Olympus); 70 nm serial sections of these regions of interest were cut with an Ultracut UCT ultramicrotome (Leica Microsystems) equipped with an Ultra

45° diamond knife (Diatome) and collected on pioloform-coated copper slot grids (#EMS2010-Cu, Science Services). If not otherwise stated, all chemicals were purchased from EMS - Electron Microscopy Sciences and sold by Science Services.

Electron microscopy imaging of serial sections and 3D reconstructions

Synapses were identified and imaged at 20 kx using a EM 900 Transmission Electron Microscope (Carl Zeiss, RRID:SCR_021364) operated at 80 keV and equipped with a Proscan 2K Slow-Scan CCD-Camera (Carl Zeiss). The *stratum lucidum* of the hippocampal region CA3 was easily distinguishable for the presence of big mossy fiber *boutons* and for its localization just above the pyramidal cell layer. Serial images of individual mossy fiber *boutons* were manually acquired in manually collected serial sections using the ImageSP software (TRS & SysProg) and aligned using the Midas script of the IMOD Software (RRID:SCR_003297). ImageSP software is commercially available at https://sys-prog.com/en/software-for-science/imagesp/ and IMOD software is freely available at https://bio3d.colorado.edu/imod/. Synaptic profiles were manually segmented in each image of series belonging to the same mossy fiber *bouton*. Active zones were traced in IMOD as open lines in serial projections and rendered as a meshed surface. The volume of the 3D reconstruction was calculated by creating a meshed 3D volume in IMOD.

Synaptic vesicle analysis

To analyze synaptic vesicles, we used a machine-learning-based algorithm that we had previously developed (Imbrosci et al., 2022). It is freely available at https://github.com/Imbrosci/synaptic-vesicles-detection-extra. Briefly, we manually traced the contour of the mossy fiber *bouton* using Fiji (RRID:SCR_002285), freely available at https://fiji.sc/. This approach allowed us to obtain a measure of the *bouton* area and to create a mask over parts of the image which were not relevant for analysis. Synaptic vesicle analysis was performed automatically in a batch. From all images the number of vesicles as well as the mean nearest neighbor distance were obtained. A tutorial with a demonstration of the tool can be found online at https://www.youtube.com/watch?v=cvqIcFldVPw.

Statistics

For statistical analysis we used GraphPad Prism software (GraphPad Prism version 8.4.0 for Windows, San Diego, California USA (RRID:SCR_002798)) and R Project for Statistical Computing (version 4.2.2, RRID:SCR_001905) in RStudio (version 2022.12.0, RRID:SCR_000432). GraphPad prism is commercially available at https://www.graphpad.com/ and R Project for Statistical Computing is freely available at https://www.r-project.org/. Data were visually inspected and tested for normality (D'Agostino and Pearson test) before evaluating them statistically, to understand if the distribution was Gaussian or non-Gaussian. Individual data points are shown as median +/- quartiles, mean values with borders of 95% confidence intervals or as mean +/- SEM.

GraphPad Prism

For Figure 1b and Figure 1-1b, data points were fitted with a simple linear regression. Slopes of those regressions were tested with a two-tailed ANCOVA and are shown with 95% confidence bands. For Figure 1c, Figure 1-1c, Figure 2b+e and Figure 3a+c, data were tested with a mixed-effects model and a post-hoc Sidak's test for multiple comparisons. Factors time, genotype and the interaction of both were tested. For Figure 1d, Figure 1-1d, Figure 1-2a-c, Figure 2c+f, Figure 2-1c and Figure 3d, ranks were compared with Mann-Whitney *U* tests. For data in Figure 3b we used a Kruskal-Wallis test with a post-hoc Dunn's correction for multiple comparisons. For Figure 2-1b we used a Wilcoxon test to compare ranks.

R Project for Statistical Computing in RStudio

To account for the multi-level nested structure of the electron microscopy data (Figure 4c,d and Figure 5b), we used a generalized linear mixed model from the gamma family with a log link. We used the glmer function from the R package: lme4 (RRID:SCR_015654) (Bates et al., 2015) to fit the generalized linear mixed models. The different models were compared with an ANOVA. In case of the data underlying Figure 5b we performed a post-hoc test (estimated marginal means with false discovery rate correction) for multiple comparisons. To obtain the marginal means we used the R package: emmeans (RRID:SCR_018734) and compared them in a marginal effects test with false discovery rate correction (Benjamini and Hochberg, 1995).

Results

Mossy fibers of SynTKO animals are more excitable

Despite the sparse connectivity (Amaral et al., 1990) and the low baseline activity of granule cells (Jung and McNaughton, 1993), a single mossy fiber *bouton* is able to trigger the discharge of its postsynaptic partner (Henze et al., 2002; Vyleta et al., 2016). Mossy fiber activity is not only important for pattern separation in the healthy brain (Rolls, 2018), but also for propagation of seizures in the epileptic brain (Nadler, 2003). Since SynTKO animals display high network excitability and develop epileptic seizures at the age of two months (Gitler et al., 2004; Fassio et al., 2011), we tested the excitability in mossy fibers by measuring the input-output relationship. We performed experiments in presymptomatic (4-6 weeks old) and symptomatic (17-19 weeks old) animals, after the onset of epileptic seizures. This design was aimed at differentiating changes in synaptic transmission that could lead to or result from epilepsy in SynTKO animals.

We conducted field recordings in acute slices from SynTKO and wildtype (WT) age-matched controls and recorded the input-output relationship as a measure of synaptic strength. We recorded from the *stratum lucidum* of area CA3 while stimulating close to the granule cell layer in the hilus (Figure 1a). We found that SynTKO were significantly more excitable than WT animals: the input-output relation was increased in both 4-6 weeks old (Figure 1b) and 17-19 weeks old animals (Figure 1-1b). With the same amount of stimulated fibers (size of the presynaptic fiber volley), the excitatory postsynaptic field potential (fEPSP) amplitudes were larger. The slopes of the simple linear regression fits of fiber volley versus fEPSP amplitudes were significantly different with $p < 0.0001$ between control and SynTKO data for both age groups. For presymptomatic recordings the slopes for the simple linear regression with 95% confidence intervals were 0.106 [0.018 – 0.194] for WT and 2.743 [2.159 – 3.326] for SynTKO and for symptomatic recordings 0.795 [0.59 – 0.99] for WT and 2.292 [1.806 – 2.777] for SynTKO.

The possible reasons underlying this increased excitability are manifold. Since the hippocampal morphology was described to be similar between WT and SynTKO animals (Gitler et al., 2004), we assume that the number of excitable fibers is comparable. To check for a possible change in release probability, we measured the paired-pulse ratio (PPR) with an inter-stimulus interval of 50 ms. Under

our experimental conditions the PPR was not significantly different between presymptomatic SynTKO and WT animals (Figure 1-2a). In WT recordings the median PPR was 2.962 [2.510; 3.960], while in recordings from SynTKO it was 3.745 [2.422; 5.570] with a p-value > 0.2 (Mann-Whitney *U* test). However, we saw a trend for an increased PPR that became clearer with a shortening of the inter-stimulus interval to 40 ms (see first two fEPSPs in Figure 2a,b). Here, in WT recordings, the median PPR was 3.833 [2.654; 4.026], while it was 4.436 [3.485; 6.094] for SynTKO (Figure 1-2b). The p-value was 0.14 (Mann-Whitney *U* test). Finally, in symptomatic SynTKO animals, the PPR was significantly increased compared to WT animals with p = 0.03 (Mann-Whitney *U* test) with a median of 2.906 [2.549; 3.499] for WT and 3.435 [2.964; 4.944] for SynTKO animals (Figure 1-2c). A change in PPR is suggestive of a change in release probability (Dobrunz and Stevens, 1997); however, this might be taken with caution as many other factors affect this measure (Hanse and Gustafsson, 2001; Sun et al., 2005; Neher and Brose, 2018; Glasgow et al., 2019).

Reduced frequency facilitation in mossy fibers of SynTKO animals

Mossy fiber *boutons* are very powerful synapses when it comes to presynaptic plasticity. They are able to facilitate dramatically, even at moderate frequencies (Salin et al., 1996). This phenotype, together with large pools of synaptic vesicles (Hallermann et al., 2003; Rollenhagen et al., 2007), makes them an excellent system for studying the influence of synapsins on presynaptic plasticity. In previous work, it has been reported that frequency facilitation is impaired at mossy fibers from SynDKO animals after stimulation with a moderate frequency of 2 Hz (Owe et al., 2009). The authors suggested that the remaining synapsin isoform – SynIII – causes impaired facilitation since it was localized in the RRP of mossy fiber *boutons*. Additionally, neurons from SynIII KO animals show less synaptic depression than WT neurons in primary hippocampal cultures (Feng et al., 2002). Here, we intended to test if complete deletion of synapsins, including SynIII, would rescue frequency facilitation at the hippocampal mossy fiber *bouton*.

When stimulated with a train of 20 pulses at a frequency of 1 Hz, we saw less facilitation in mossy fibers from presymptomatic SynTKO compared to WT animals. This finding is comparable to the aforementioned experiments in SynDKO animals (Owe et al., 2009) and cell culture experiments of

406 SynTKO animals (Gitler et al., 2004). The rise in the field excitatory postsynaptic potential (fEPSP)
407 amplitudes was similar in WT and SynTKO during the first 10 stimuli, but in SynTKO animals we
408 observed an earlier saturation of amplitudes. In SynTKO the amplitudes reached a plateau after 15
409 stimuli, whereas in WT animals the amplitudes increased until the end of the 1 Hz stimulation (Figure
410 1c). When comparing the plots with a mixed-effects model, we found significant differences for the
411 factor time, as well as for the interaction between time and genotype ($p < 0.0001$). The post-hoc Sidak's
412 test for multiple comparisons revealed no significant differences for single time points ($p > 0.05$). When
413 comparing only the amplitudes in response to the last 1 Hz stimulus, we found that the median
414 facilitation was 6.909 [5.589; 9.093] for WT animals, while the increase was only 5.110 [3.760; 7.080]
415 compared to the baseline for SynTKO animals (median value [25% quartile; 75% quartile]). Ranks were
416 different with $p = 0.0029$ (Mann-Whitney *U* test (Figure 1d)).

417 This result suggests that SynIII is not the primary reason for the reduced facilitation in mossy fiber
418 *boutons*. However, Owe and coworkers used three to six months old SynDKO mice. Since all synapsin
419 knockout animals lacking SynI and/or SynII develop seizures beginning at the age of two months (Fassio
420 et al., 2011), this pathology could potentially lead to secondary differences in plasticity. We investigated
421 short-term plasticity also in 17-19 weeks old symptomatic mice – matching the age range from Owe et
422 al. – and observed an even more pronounced effect on frequency facilitation (Figure 1-1c,d): the
423 facilitation in WT animals reached 7.019 [5.574; 8.440] while the increase in SynTKO recordings was
424 only 4.414 [4.036; 5.330] compared to baseline (median [25% quartile; 75% quartile]). Ranks were
425 significantly different with $p = 0.0009$ (Mann-Whitney *U* test). Thus, the additional knockout of SynIII
426 did not lead to a rescue of facilitation, neither in presymptomatic nor in symptomatic animals. Hence,
427 our data do not support the hypothesis that SynIII acts as a brake on frequency facilitation in
428 hippocampal mossy fiber *boutons*.

429 In summary, we see a decrease in frequency facilitation, but an increase in excitability in the absence of
430 synapsins. These results indicate that, (1) SynIII is not causing the reduced facilitation and (2) that before
431 the onset of epileptic seizures, excitability and short-term plasticity mechanisms are already altered.

High-frequency stimulation leads to early vesicle exhaustion in SynTKO animals

Since stimulation with a moderate frequency led to a decrease in facilitation in presymptomatic SynTKO animals (Figure 1c,d), we wanted to investigate the response to a longer stimulation with a higher frequency. We applied four trains of 125 pulses at 25 Hz using the same recording paradigm as before (Figure 1a). While the course of the amplitudes was very similar in the first high-frequency train for both genotypes (Figure 2a,b,c), changes manifested over time. Differences between WT and SynTKO animals became distinguishable in the fourth stimulation train (Figure 2d,e,f) with smaller amplitudes throughout the whole train in SynTKO animals.

When tested with a mixed-effects model, we detected significant differences for the factor time (stimuli) for both the first and the fourth stimulation train ($p < 0.0001$). The factor genotype and the interaction of genotype and time were only significant for the fourth stimulation train ($p < 0.05$). A post-hoc Sidak's test for multiple comparisons revealed no significant differences for single time points for either of the stimulation trains. We also compared the amplitudes for the last stimulus of the stimulation trains between genotypes. For the first stimulation train, the median normalized fEPSP amplitude was 1.848 [1.243; 2.467] for WT, while it was 0.7514 [0.4997; 1.650] for SynTKO animals. Ranks were not significantly different ($p = 0.1956$; Mann-Whitney *U* test) (Figure 2c). However, when comparing the amplitudes of the last stimulus of the fourth stimulation train, we found a significant difference ($p = 0.0037$, Mann-Whitney *U* test) between WT and SynTKO (Figure 2f). The median normalized fEPSP amplitude was 1.381 [0.6876; 2.293] for WT and 0.3714 [0.04892; 0.7202] for SynTKO animals. This stronger exhaustion during intense stimulation was already described before in other synapsin knockout animals (Rosahl et al., 1995; Farisello et al., 2013) and probably reflects the missing reserve pool, which would normally replenish the RRP under such high activity (Vasileva et al., 2012).

High-frequency stimulation can lead to a loss of fibers during the course of stimulation. To check if the smaller fEPSP amplitudes in the last stimulation train of SynTKO recordings is due to an increased fiber loss, we measured a subset of the presynaptic fiber volleys (PFV) during the first and fourth stimulation train for both genotypes, respectively. While PFVs of SynTKO animals were in general smaller than the ones from WT animals with comparable fEPSP amplitudes (Figure 1b), there was no relative difference

in PFV sizes of the two genotypes between first and last stimulation train (Figure 2-1). Thus, we conclude that the relative loss of fibers is similar for both genotypes and does not explain the more drastic decrease in fEPSP size for SynTKO animals.

Here, our data indicate that deletion of all synapsins disturbs the vesicle organization in synaptic terminals in a way that leads to impaired replenishment. This is especially relevant for synapses like mossy fiber *boutons*, which have large vesicle pools (Hallermann et al., 2003; Rollenhagen et al., 2007).

Post-tetanic potentiation is changed in SynTKO animals

After intense stimulation of mossy fibers, another form of short-term plasticity occurs: post-tetanic potentiation (PTP) (Griffith, 1990), which was proposed to underlie short-term memory (Vandael et al., 2020). Measuring PTP after four trains of high-frequency stimulation revealed differences between WT and SynTKO animals: while in WT recordings the median potentiation was 7.234 [6.752; 8.478] fold compared to baseline and decreased over time, in SynTKO recordings, we initially measured an amplitude which was only 3.702 [2.683; 5.280] times larger than baseline (significantly different in a Kruskal-Wallis test with post-hoc Dunn's test for multiple comparisons; $p = 0.0002$), but increased over time. After one minute, the amplitudes of WT and SynTKO recordings were comparable (Figure 3a,b; WT: 5.323 [4.070; 6.812]; SynTKO: 4.887 [3.769; 6.419]; $p > 0.99$), followed by a further increase in the SynTKO amplitudes over WT amplitudes. One minute after stimulation, the amplitudes of the SynTKO animals remained on a plateau while the amplitudes in the WT animals decreased further (Figure 3a,b), leading to median amplitudes of 2.717 [2.432; 2.922] for WT and 4.865 [3.635; 6.497] for SynTKO animals approximately three minutes after high-frequency stimulation (significantly different with $p = 0.001$). These findings point to different underlying mechanisms: one leading to the impairment of PTP right after high-frequency stimulation and another one leading to increased amplitudes after some recovery time and upon low frequency stimulation of 0.05 Hz. To understand this observation further, we continued recording for half an hour, which corresponds to early long-term potentiation (LTP).

Long-term potentiation is enhanced in SynTKO animals

Mossy fiber *boutons* express a presynaptic form of LTP, which is PKA-dependent (Weisskopf et al., 1994). In recordings from SynDKO animals mossy fiber LTP was unchanged compared to WT animals (Spillane et al., 1995). It is tempting to speculate, though, that SynIII might be the phosphorylation target of PKA in the context of LTP, since a PKA phosphorylation site is present in domain A (Piccini et al., 2015), which is conserved among all synapsins, and SynIII expression is maintained in adult mossy fiber *boutons* (Pieribone et al., 2002). An additional knockout of SynIII could therefore lead to a block of LTP. However, when recording long-term potentiation (Figure 3c) we measured a median potentiation of 1.43 [1.23; 1.77] in WT animals 20 to 30 minutes after the high-frequency stimulation, while SynTKO animals showed a larger median potentiation of 2.45 [1.98; 3.12] compared to baseline (Figure 3d). Ranks differed significantly with $p < 0.0001$ (Mann-Whitney *U* test). The time course of LTP was tested in a mixed-effects model. The factors genotype, time and the interaction of both differed significantly ($p = 0.013$; $p < 0.0001$; $p < 0.0001$, respectively). A post-hoc Sidak's test for multiple comparisons revealed significant differences for single time points as well (Figure 3c). We included all measurements that fulfilled the specificity criterion, which was tested by the application of the metabotropic glutamate receptor group II agonist (2*S*,1'*R*,2'*R*,3'*R*)-2-(2,3-dicarboxycyclopropyl)glycine (DCG-IV) (Kamiya et al., 1996) (last ten sweeps are shown in Figure 3c).

In summary, the absence of all synapsin isoforms in mossy fiber synapses leads to a reduced early PTP, an altered time-course of PTP/LTP and an increased long-lasting potentiation. Such changes in LTP have not been described before in other synapsin knockout models, suggesting that it is an effect of SynIII deletion and specifically relevant for the mossy fiber *bouton,* where LTP occurs presynaptically (Zalutsky and Nicoll, 1990). Since it has been shown that ultrastructural changes underlie potentiation at hippocampal mossy fibers (Orlando et al., 2021) we next sought to investigate the ultrastructure of mossy fiber *boutons* in SynTKO animals.

Synaptic vesicles are more dispersed in SynTKO animals

So far, vesicle distributions at the hippocampal mossy fiber *bouton* have only been described for either SynDKO animals or SynIII KO animals (Feng et al., 2002; Owe et al., 2009). Here, we wanted to test whether the knockout of all three synapsins would lead to additional changes in vesicle organization at the hippocampal mossy fiber *bouton*. Using transmission electron microscopy (TEM), we identified individual mossy fiber *boutons* from three presymptomatic SynTKO and two age-matched WT mice. We imaged serial sections from 16 SynTKO and 12 WT mossy fiber *boutons*. For each 2D projection, we measured the vesicle number and the mean nearest neighbor distance (MNND) using an automated tool (Imbrosci et al., 2022) (Figure 4a). For both data sets, we used a generalized linear mixed model (gamma family with log link) to predict either the vesicle density or MNND. When comparing synaptic vesicles of WT and SynTKO *boutons*, the mean density was strongly reduced in *boutons* from SynTKO animals (687 [532; 886] vesicles/μm^3 compared to 2186 [1612; 2965] vesicles/μm^3 in WT) (Figure 4b,c). The genotypes were significantly different with $p = 0.006$. Consequently, we also saw an increase in the MNND of vesicles (Figure 4b,d): the average MNND was 56.3 [52.3; 60.6] nm for WT and 101.2 [95.1; 107.8] nm for SynTKO *boutons*. Groups were significantly different with $p = 0.0015$. The reduced density of distal vesicles implies a reduced reserve pool. Since this observation resembles the results seen in mossy fiber *boutons* of SynDKO animals (Owe et al., 2009), our data indicate that the additional knockout of SynIII does not add on effects on the organization of the distal pool. This conclusion is also in line with unchanged synaptic vesicle densities in mossy fiber *boutons* of SynIII KO mice (Feng et al., 2002).

Active zone density is highest in chemically potentiated mossy fiber *boutons* from SynTKO animals

Since we saw an increase in LTP in SynTKO animals (Figure 3c,d), we wanted to understand if structural changes would occur in potentiated mossy fiber *boutons* from SynTKO animals. We performed TEM in hippocampal slices from both young WT and SynTKO animals in either potentiated or control conditions. Potentiation was chemically induced via incubation with the adenylyl cyclase-activator forskolin before fixation of the samples. Forskolin has similar effects on mossy fibers as high-

frequency electrical stimulation (Weisskopf et al., 1994; Spillane et al., 1995). The active zone density was analyzed in partial 3D reconstructions of mossy fiber *boutons* from three animals per group and replicates of 17 (WT), 16 (WT + forskolin), 16 (SynTKO) and 18 (SynTKO + forskolin) *boutons*, respectively. We fitted a generalized linear mixed model (gamma family with a log link) to predict active zone density with genotype and forskolin treatment, which included the individual animals as random effects. We found significant differences for genotype ($p = 0.01$) and forskolin treatment ($p = 0.013$). Specific pairs were compared by testing estimated marginal means with adjustment for false discovery rate (Benjamini and Hochberg, 1995).

We observed an increase in the active zone density in WT animals when treated with forskolin, as described before (Orlando et al., 2021). Untreated *boutons* from SynTKO animals had a similar mean density of active zones as forskolin-treated *boutons* from WT animals (5.63 [4.43; 7.14] active zones/μm^3 for untreated SynTKO *boutons*; 5.22 [4.13; 6.60] active zones/μm^3 for forskolin-treated WT *boutons,* $p = 0.658$). This indicates that, from a structural point of view, SynTKO animals could be in a similar state as potentiated WT *boutons*. Treatment with forskolin led to a further increase in the active zone density in mossy fiber *boutons* from SynTKO animals (10.20 [7.50; 13.88] active zones/μm^3) (Figure 5a) and led to significant differences when compared to untreated SynTKO *boutons* ($p = 0.0018$) as well as treated WT *boutons* ($p = 0.0018$) (Figure 5b). Taken together, we might see a structural strengthening in *boutons* from SynTKO animals treated with forskolin, which could explain the increase in long-term potentiation (Figure 3c,d).

Discussion

Here, we demonstrate that synapsin-dependent vesicle organization plays a crucial role in various forms of presynaptic plasticity at hippocampal mossy fiber *boutons*. The removal of all synapsin isoforms leads to impaired PTP, indicating a potential role of synapsins in short-term memory. Active zone density was increased in mossy fiber *boutons* of SynTKO animals, indicating a preset potentiated state. This morphological phenotype might underlie the increased LTP we observed in SynTKO animals.

Together, our results indicate that all synapsin isoforms, including SynIII, play a role in the modulation of mossy fiber-specific presynaptic plasticity.

In SynTKO mice, we found increased excitability, measured by a change in the input-output relation of local fEPSPs (Figure 1, Figure 1-1). A likely explanation is based on the finding that synapsins play different roles in excitatory versus inhibitory neurons (Song and Augustine, 2015). Deletion or mutation of SynI, SynIII or all synapsins leads to impaired basal transmission of inhibitory, but not excitatory cultured neurons (Terada et al., 1999; Feng et al., 2002; Gitler et al., 2004; Baldelli et al., 2007) and loss of SynII impairs tonic inhibition in hippocampal slices (Medrihan et al., 2013, 2015). Mossy fibers activate at least four times more inhibitory neurons than pyramidal cells in CA3 (Acsády et al., 1998), regulating CA3 excitability via feedforward inhibition (Acsády and Káli, 2007; Torborg et al., 2010). Reduced feedforward inhibition might thus explain the increased excitability. Indeed, the input-output relation is increased in Schaffer collaterals from SynTKO animals, while it is reduced in inhibitory fibers from CA1 (Farisello et al., 2013).

During trains of activity, mossy fiber *boutons* facilitate reliably (Salin et al., 1996; Toth et al., 2000), which is thought to be important for information transfer (Henze et al., 2002; Mori et al., 2004). In mossy fibers from SynDKO animals, frequency facilitation is reduced (Owe et al., 2009). There, the authors suggested that the remaining SynIII may act as a brake on facilitation, because (1) SynIII is associated specifically with the RRP in mossy fiber *boutons* (Owe et al., 2009) and (2) synaptic depression is reduced in SynIII KO cultures (Feng et al., 2002). However, in animals lacking all synapsins, including SynIII, we still observed reduced frequency facilitation (Figure 1, Figure 1-1), rejecting the hypothesis from Owe and colleagues. Frequency facilitation is most likely calcium-dependent and involves increased neurotransmitter release (Chamberland et al., 2017; Jackman and Regehr, 2017). Hence, potential reasons for reduced facilitation are diverse and include enhanced basal release probability, depletion of the RRP and saturation of postsynaptic receptors (Neher and Sakaba, 2008).

High-frequency stimulation usually results in a biphasic depression, attributed to the depletion of the RRP (Zucker and Regehr, 2002) and slow replenishment from the reserve pool (Wesseling and Lo,

2002). We observed frequency-dependent depression for both genotypes when stimulating at 25 Hz (Figure 2), but stronger depression in SynTKO animals, recapitulating previous results (Gitler et al., 2004). At the calyx of Held, a reduced reserve pool and slower replenishment accounted for faster depression in SynTKO animals (Vasileva et al., 2012). Indeed, in mossy fiber *boutons* of SynTKO animals, vesicles in the distal pool were reduced in density and more dispersed (Figure 4), likely explaining faster depression. Impaired distal pools were described before for mossy fiber *boutons* (Takei et al., 1995; Owe et al., 2009) and in neuronal cultures from SynTKO mice (Gitler et al., 2004; Siksou et al., 2007). Hence, at mossy fibers, the additional knockout of SynIII recapitulates previously described phenotypes – in line with unchanged reserve pools in SynIII KO mossy fiber *boutons* (Feng et al., 2002) and a role of SynIIa in vesicle replenishment (Gitler et al., 2008). In general, vesicle de-clustering and reduced vesicle density likely have diverse effects on the release cycle (Bykhovskaia, 2011), possibly also supporting increased excitability and reduced frequency facilitation.

PTP has recently been suggested to underlie short-term memory. During mossy fiber PTP a "pool engram" is formed, i.e. the number of docked vesicles at active zones increases (Vandael et al., 2020). This engram formation depends on the refilling rate of vesicles and could thus be mediated by synapsins. Our data support this hypothesis: the complete loss of synapsins impairs mossy fiber PTP (Figure 3). Reduced PTP was observed before in synapsin KO models, with diversity regarding synapsin isoform and synapse type. PTP is reduced in (1) cultured hippocampal neurons of SynI KO and SynTKO animals (Valente et al., 2012; Cheng et al., 2018), (2) at Schaffer collaterals of SynII KO, SynDKO and SynTKO animals (Rosahl et al., 1995; Farisello et al., 2013) and (3) at corticothalamic synapses of SynI, but not SynII, KO animals (Nikolaev and Heggelund, 2015). However, no change in PTP was reported for mossy fibers of SynDKO animals (Spillane et al., 1995). We therefore speculate that the lack of SynIII in SynTKO mice might cause the additional PTP phenotype that we observe in mossy fibers. In cell culture, PTP measured via miniature excitatory postsynaptic currents could only be rescued by the SynIIIa isoform (Cheng et al., 2018), supporting this notion.

While the initial drop in PTP could be explained by impaired vesicle replenishment (Vasileva et al., 2012), we also observed a second, increased PTP phase (Figure 3a,b). Alongside the RRP, also release

probability and quantal size are increased during mossy fiber PTP (Vandael et al., 2020). Both could be elevated by default in SynTKO animals and elevate PTP in the second phase. Interestingly, we detected an increase in active zone density in SynTKO *boutons* (Figure 5), which most likely reflects a change in the number of release sites. Hence, after overcoming the initial drop in PTP, other mechanisms could be untamed in SynTKO mossy fiber *boutons*, leading to enhanced PTP in a later phase.

We discovered previously that active zone density is increased in potentiated mossy fiber *boutons* (Orlando et al., 2021). Therefore, the increased density in SynTKO animals could indicate a preset potentiated state due to homeostatic adaptation, similar to mechanisms in the calyx of Held of SynTKO animals (Vasileva et al., 2012). The active zone density was further increased when chemically potentiating SynTKO mossy fibers with forskolin, leading to significantly higher densities than in forskolin-treated WT *boutons* and untreated SynTKO *boutons* (Figure 5). Forskolin could induce these structural changes via SynIII phosphorylation by PKA, similar to developmental processes (Piccini et al., 2015). Elevated active zone densities might also explain the increased LTP we observe in SynTKO animals (Figure 3). Mossy fiber LTP was analyzed before in SynI KO (Takei et al., 1995) and SynDKO mice (Spillane et al., 1995), but was found to be unchanged. Thus, we speculate that the increase in LTP is a likely consequence of the additional knockout of SynIII.

It is unknown which mechanisms are shared between mossy fiber PTP and LTP and when one results in the other. SynIII might have a specific function in both processes, preventing excess release and balancing potentiation. Recent literature suggests that (1) diversity in STP depends on priming and fusion steps (Lin et al., 2022) and (2) increased fusion competence might underlie mossy fiber LTP, possibly mediated by Munc13-1 (Lipstein et al., 2021; Fukaya et al., 2023a; Papantoniou et al., 2023). Does SynIII play a role in the insertion of new active zones, vesicle docking, priming and/or fusion? Such a role would most likely be intermingled with SynIIIs role in neurogenesis (Kao et al., 2008). Future work in SynIII KO models will allow us to answer this question.

Here, we investigated plasticity at a glutamatergic synapse expressing SynIII in adulthood. We used SynTKO instead of SynIII KO animals to exclude compensatory effects via remaining synapsin isoforms. However, this approach also limits our ability to draw precise conclusions on SynIII-specific

644 effects. By combining physiological recordings – well-suited to record mossy fiber transmission
645 (Breustedt et al., 2010) – and ultrastructural studies, our experiments shed light on synapsin-dependent
646 plasticity from different angles. To exclude possible indirect estrogen-effects on mossy fiber plasticity
647 (Harte-Hargrove et al., 2013), we used male mice only, limiting the generalizability. Future studies
648 should include female animals. Finally, although chemical mossy fiber potentiation is widely used, it is
649 still unclear if it shares the same mechanisms as electrical induction (Shahoha et al., 2022; Fukaya et al.,
650 2023b).

651 Our work revealed that the complete loss of synapsins leads to disruption of presynaptic plasticity at
652 hippocampal mossy fibers. Facilitation and PTP are reduced, likely due to an impaired vesicle
653 replenishment. However, LTP is increased, in concert with an elevated active zone density. We speculate
654 that the loss of SynIII supports these physiological and ultrastructural changes. Our work contributes to
655 a better understanding of mossy fiber presynaptic plasticity and, consequently, to a better understanding
656 of synapsins' roles in learning and memory. Further work is needed to dissect the precise roles of the
657 various synapsin isoforms both in hippocampal mossy fiber *boutons* and in other synapses, especially
658 those expressing SynIII in adult stages (Pieribone et al., 2002).

659 # References

660 Acsády L, Káli S (2007) Models, structure, function: the transformation of cortical signals in the
661 dentate gyrus. Prog Brain Res 163:577–599.

662 Acsády L, Kamondi A, Sík A, Freund T, Buzsáki G (1998) GABAergic cells are the major
663 postsynaptic targets of mossy fibers in the rat hippocampus. J Neurosci 18:3386–3403.

664 Amaral DG, Ishizuka N, Claiborne B (1990) Chapter Neurons, numbers and the hippocampal network.
665 Prog Brain Res 83:1–11.

666 Atias M, Tevet Y, Sun J, Stavsky A, Tal S, Kahn J, Roy S, Gitler D (2019) Synapsins regulate α-
667 synuclein functions. Proc Natl Acad Sci U S A 166:11116–11118.

668 Baldelli P, Fassio A, Valtorta F, Benfenati F (2007) Lack of synapsin I reduces the readily releasable
669 pool of synaptic vesicles at central inhibitory synapses. J Neurosci 27:13520–13531.

670 Bates D, Mächler M, Bolker BM, Walker SC (2015) Fitting linear mixed-effects models using lme4. J
671 Stat Softw 67.

672 Benjamini Y, Hochberg Y (1995) Controlling the False Discovery Rate: A Practical and Powerful
673 Approach to Multiple Testing. J R Stat Soc Ser B 57:289–300.

674 Breustedt J, Gundlfinger A, Varoqueaux F, Reim K, Brose N, Schmitz D (2010) Munc13-2
675 differentially affects hippocampal synaptic transmission and plasticity. Cereb Cortex 20:1109–1120.

676 Browning MD, Huang CK, Greengard P (1987) Similarities between protein IIIa and protein IIIb, two
677 prominent synaptic vesicle-associated phosphoproteins. J Neurosci 7:847–853.

678 Bykhovskaia M (2011) Synapsin regulation of vesicle organization and functional pools. Semin Cell
679 Dev Biol 22:387–392.

680 Cesca F, Baldelli P, Valtorta F, Benfenati F (2010) The synapsins: Key actors of synapse function and
681 plasticity. Prog Neurobiol 91:313–348.

682 Chamberland S, Evstratova A, Tóth K (2017) Short-term facilitation at a detonator synapse requires
683 the distinct contribution of multiple types of voltage-gated calcium channels. J Neurosci 37:4913–
684 4927.

685 Cheng Q, Song S, Augustine GJ (2018) Molecular Mechanisms of Short-Term Plasticity: Role of
686 Synapsin Phosphorylation in Augmentation and Potentiation of Spontaneous Glutamate Release. Front
687 Synaptic Neurosci 10:1–12.

688 Chi P, Greengard P, Ryan TA (2001) Synapsin dispersion and reclustering during synaptic activity.
689 Nat Neurosci 4:1187–1193.

690 De Camilli P, Benfenati F, Valtorta F, Greengard P (1990) The synapsins. Annu Rev Cell Biol 6:433–
691 460.

692 De Camilli P, Cameron R, Greengard P (1983) Synapsin I (protein I), a nerve terminal-specific
693 phosphoprotein. I. Its general distribution in synapses of the central and peripheral nervous system
694 demonstrated by immunofluorescence in frozen and plastic sections. J Cell Biol 96:1337–1354.

695 Dobrunz LE, Stevens CF (1997) Heterogeneity of release probability, facilitation, and depletion at
696 central synapses. Neuron 18:995–1008.

697 Farisello P, Boido D, Nieus T, Medrihan L, Cesca F, Valtorta F, Baldelli P, Benfenati F (2013)
698 Synaptic and extrasynaptic origin of the excitation/inhibition imbalance in the hippocampus of
699 synapsin I/II/III knockout mice. Cereb Cortex 23:581–593.

700 Fassio A, Raimondi A, Lignani G, Benfenati F, Baldelli P (2011) Synapsins: From synapse to network
701 hyperexcitability and epilepsy. Semin Cell Dev Biol 22:408–415.

702 Feng J, Chi P, Blanpied TA, Xu Y, Magarinos AM, Ferreira A, Takahashi RH, Kao HT, McEwen BS,
703 Ryan TA, Augustine GJ, Greengard P (2002) Regulation of Neurotransmitter Release by Synapsin III.
704 J Neurosci 22:4372–4380.

705 Ferreira A, Kao HT, Feng J, Rapoport M, Greengard P (2000) Synapsin III: Developmental
706 expression, subcellular localization, and role in axon formation. J Neurosci 20:3736–3744.

707 Fukaya R, Hirai H, Sakamoto H, Hashimotodani Y, Hirose K, Sakaba T (2023a) Increased vesicle
708 fusion competence underlies long-term potentiation at hippocampal mossy fiber synapses. Sci Adv
709 9:1–14.

710 Fukaya R, Miyano R, Hirai H, Sakaba T (2023b) Mechanistic insights into cAMP-mediated
711 presynaptic potentiation at hippocampal mossy fiber synapses. Front Cell Neurosci 17:1–8.

712 Gitler D, Cheng Q, Greengard P, Augustine GJ (2008) Synapsin IIa controls the reserve pool of
713 glutamatergic synaptic vesicles. J Neurosci 28:10835–10843.

714 Gitler D, Takagishi Y, Feng J, Ren Y, Rodriguiz RM, Wetsel WC, Greengard P, Augustine GJ (2004)
715 Different presynaptic roles of synapsins at excitatory and inhibitory synapses. J Neurosci 24:11368–
716 11380.

717 Glasgow SD, McPhedrain R, Madranges JF, Kennedy TE, Ruthazer ES (2019) Approaches and
718 limitations in the investigation of synaptic transmission and plasticity. Front Synaptic Neurosci 11:1–
719 16.

720 Griffith WH (1990) Voltage-clamp analysis of posttetanic potentiation of the mossy fiber to CA3
721 synapse in hippocampus. J Neurophysiol 63:491–501.

722 Hallermann S, Pawlu C, Jonas P, Heckmann M (2003) A large pool of releasable vesicles in a cortical
723 glutamatergic synapse. Proc Natl Acad Sci U S A 100:8975–8980.

724 Hanse E, Gustafsson B (2001) Paired-pulse plasticity at the single release site level: An experimental
725 and computational study. J Neurosci 21:8362–8369.

726 Harte-Hargrove LC, MacLusky NJ, Scharfman HE (2013) Brain-derived neurotrophic factor-estrogen
727 interactions in the hippocampal mossy fiber pathway: Implications for normal brain function and
728 disease. Neuroscience 239:46-66.

729 Heidari S, Babor TF, De Castro P, Tort S, Curno M (2016) Sex and Gender Equity in Research:
730 rationale for the SAGER guidelines and recommended use. Res Integr Peer Rev 1:1–9.

731 Henze DA, Wittner L, Buzsáki G (2002) Single granule cells reliably discharge targets in the
732 hippocampal CA3 network in vivo. Nat Neurosci 5:790–795.

733 Hirokawa N, Sobue K, Kanda K, Harada A, Yorifuji H (1989) The cytoskeletal architecture of the
734 presynaptic terminal and molecular structure of synapsin 1. J Cell Biol 108:111–126.

735 Hosaka M, Hammer RE, Südhof TC (1999) A phospho-switch controls the dynamic association of
736 synapsins with synaptic vesicles. Neuron 24:377–387.

737 Imbrosci B, Schmitz D, Orlando M (2022) Automated detection and localization of synaptic vesicles
738 in electron microscopy images. eNeuro 9:1–16.

739 Jackman SL, Regehr WG (2017) The Mechanisms and Functions of Synaptic Facilitation. Neuron
740 94:447–464.

741 Jung MW, McNaughton BL (1993) Spatial selectivity of unit activity in the hippocampal granular
742 layer. Hippocampus 3:165–182.

743 Kamiya H, Shinozaki H, Yamamoto C (1996) Activation of metabotropic glutamate receptor type 2/3
744 suppresses transmission at rat hippocampal mossy fibre synapses. J Physiol 493:447–455.

745 Kao HT, Li P, Chao HM, Janoschka S, Pham K, Feng J, Mcewen BS, Greengard P, Pieribone VA,
746 Porton B (2008) Early involvement of synapsin III in neural progenitor cell development in the adult
747 hippocampus. J Comp Neurol 507:1860–1870.

748 Kao HT, Porton B, Czernik AJ, Feng J, Yiu G, Häring M, Benfenati F, Greengard P (1998) A third
749 member of the synapsin gene family. Proc Natl Acad Sci U S A 95:4667–4672.

750 Li L, Chin LS, Shupliakov O, Brodin L, Sihra TS, Hvalby Ø, Jensen V, Zheng D, Mcnamara JO,
751 Greengard P, Andersen P (1995) Impairment of synaptic vesicle clustering and of synaptic
752 transmission, and increased seizure propensity, in synapsin I-deficient mice. Proc Natl Acad Sci U S A
753 92:9235–9239.

754 Lin KH, Taschenberger H, Neher E (2022) A sequential two-step priming scheme reproduces diversity
755 in synaptic strength and short-term plasticity. Proc Natl Acad Sci U S A 119:1–12.

756 Lipstein N, Chang S, Lin K-H, López-Murcia FJ, Neher E, Taschenberger H, Brose N (2021)
757 Munc13-1 is a Ca2+-phospholipid-dependent vesicle priming hub that shapes synaptic short-term
758 plasticity and enables sustained neurotransmission. Neuron 109:1-21.

759 Medrihan L, Cesca F, Raimondi A, Lignani G, Baldelli P, Benfenati F (2013) Synapsin II
760 desynchronizes neurotransmitter release at inhibitory synapses by interacting with presynaptic calcium
761 channels. Nat Commun 4:1512.

762 Medrihan L, Ferrea E, Greco B, Baldelli P, Benfenati F (2015) Asynchronous GABA release is a key
763 determinant of tonic inhibition and controls neuronal excitability: A study in the synapsin II-/- mouse.
764 Cereb Cortex 25:3356–3368.

765 Milovanovic D, Wu Y, Bian X, De Camilli P (2018) A liquid phase of synapsin and lipid vesicles.
766 Science 361:604–607.

767 Monday HR, Kharod SC, Yoon YJ, Singer RH, Castillo PE (2022) Presynaptic FMRP and local
768 protein synthesis support structural and functional plasticity of glutamatergic axon terminals. Neuron
769 110:1–19.

770 Monday HR, Younts TJ, Castillo PE (2018) Long-Term Plasticity of Neurotransmitter Release:
771 Emerging Mechanisms and Contributions to Brain Function and Disease. Annu. Rev. Neurosci.
772 41:299–322.

773 Mori M, Abegg MH, Gähwiler BH, Gerber U (2004) A frequency-dependent switch from inhibition to
774 excitation in a hippocampal unitary circuit. Nature 431:453–456.

775 Nadler JV (2003) The Recurrent Mossy Fiber Pathway of the Epileptic Brain. Neurochem Res
776 28:1649–1658.

777 Neher E, Brose N (2018) Dynamically Primed Synaptic Vesicle States: Key to Understand Synaptic
778 Short-Term Plasticity. Neuron 100:1283–1291.

779 Neher E, Sakaba T (2008) Multiple Roles of Calcium Ions in the Regulation of Neurotransmitter
780 Release. Neuron 59:861–872.

781 Nicoll RA, Schmitz D (2005) Synaptic plasticity at hippocampal mossy fibre synapses. Nat Rev
782 Neurosci 6:863–876.

783 Nikolaev M, Heggelund P (2015) Functions of synapsins in corticothalamic facilitation: Important
784 roles of synapsin I. J Physiol 593:4499–4510.

785 Orlando M, Dvorzhak A, Bruentgens F, Maglione M, Rost BR, Sigrist SJ, Breustedt J, Schmitz D
786 (2021) Recruitment of release sites underlies chemical presynaptic potentiation at hippocampal mossy
787 fiber boutons. PLoS Biol 19:1–29.

788 Owe SG, Jensen V, Evergren E, Ruiz A, Shupliakov O, Kullmann DM, Storm-Mathisen J, Walaas SI,
789 Hvalby O, Bergersen LH (2009) Synapsin- and Actin-Dependent Frequency Enhancement in Mouse
790 Hippocampal Mossy Fiber Synapses. Cereb Cortex 19:511–523.

791 Papantoniou C, Laugks U, Betzin J, Capitanio C, Ferrero JJ, Sánchez-Prieto J, Schoch S, Brose N,
792 Baumeister W, Cooper BH, Imig C, Lučić V (2023) Munc13- and SNAP25-dependent molecular
793 bridges play a key role in synaptic vesicle priming. Sci Adv 9:eadf6222.

794 Pechstein A, Tomilin N, Fredrich K, Vorontsova O, Sopova E, Evergren E, Haucke V, Brodin L,
795 Shupliakov O (2020) Vesicle Clustering in a Living Synapse Depends on a Synapsin Region that
796 Mediates Phase Separation. Cell Rep 30:2594-2602.e3.

797 Percie du Sert N et al. (2020) The arrive guidelines 2.0: Updated guidelines for reporting animal
798 research. PLoS Biol 18:1–12.

799 Piccini A, Perlini LE, Cancedda L, Benfenati F, Giovedì S (2015) Phosphorylation by PKA and Cdk5
800 mediates the early effects of synapsin III in neuronal morphological maturation. J Neurosci 35:13148–
801 13159.

802 Pieribone VA, Porton B, Rendon B, Feng J, Greengard P, Kao HT (2002) Expression of synapsin III
803 in nerve terminals and neurogenic regions of the adult brain. J Comp Neurol 454:105–114.

804 Pieribone VA, Shupliakov O, Brodin L, Hilfiker-Rothenfluh S, Czernik AJ, Greengard P (1995)
805 Distinct pools of synaptic vesicles in neurotransmitter release. Nature 375:493–497.

806 Rollenhagen A, Sätzler K, Rodríguez EP, Jonas P, Frotscher M, Lübke JHR (2007) Structural
807 determinants of transmission at large hippocampal mossy fiber synapses. J Neurosci 27:10434–10444.

808 Rolls ET (2018) The storage and recall of memories in the hippocampo-cortical system. Cell Tissue
809 Res 373:577–604.

810 Rosahl TW, Spillane D, Missler M, Herz J, Selig DK, Wolff JR, Hammer RE, Malenka RC, Südhof
811 TC (1995) Essential functions of synapsins I and II in synaptic vesicle regulation. Nature 375:488–
812 493.

Salin PA, Scanziani M, Malenka RC, Nicoll RA (1996) Distinct short-term plasticity at two excitatory synapses in the hippocampus. Proc Natl Acad Sci U S A 93:13304–13309.

Sansevrino R, Hoffmann C, Milovanovic D (2023) Condensate biology of synaptic vesicle clusters. Trends Neurosci 46:293–306.

Shahoha M, Cohen R, Ben-Simon Y, Ashery U (2022) cAMP-Dependent Synaptic Plasticity at the Hippocampal Mossy Fiber Terminal. Front Synaptic Neurosci 14:1–15.

Sihra TS, Wang JKT, Gorelick FS, Greengard P (1989) Translocation of synapsin I in response to depolarization of isolated nerve terminals. Proc Natl Acad Sci U S A 86:8108–8112.

Siksou L, Rostaing P, Lechaire J-P, Boudier T, Ohtsuka T, Fejtová A, Kao H-T, Greengard P, Gundelfinger ED, Triller A, Marty S (2007) Three-dimensional architecture of presynaptic terminal cytomatrix. J Neurosci 27:6868–6877.

Song S, Augustine GJ (2023) Different mechanisms of synapsin-induced vesicle clustering at inhibitory and excitatory synapses. bioRxiv 2023.03.20.533583. https://doi.org/10.1101/2023.03.20.533583

Song SH, Augustine GJ (2015) Synapsin isoforms and synaptic vesicle trafficking. Mol Cells 38:936–940.

Spillane DM, Rosahl TW, Südhof TC, Malenka RC (1995) Long-term potentiation in mice lacking synapsins. Neuropharmacology 34:1573–1579.

Südhof TC, Czernik AJ, Kao HT, Takei K, Johnston PA, Horiuchi A, Kanazir SD, Wagner MA, Perin MS, De Camilli P, Greengard P (1989) Synapsins: Mosaics of shared and individual domains in a family of synaptic vesicle phosphoproteins. Science 245:1474–1480.

Sun HY, Lyons SA, Dobrunz LE (2005) Mechanisms of target-cell specific short-term plasticity at Schaffer collateral synapses onto interneurones versus pyramidal cells in juvenile rats. J Physiol 568:815–840.

837 Takei Y, Harada A, Takeda S, Kobayashi K, Terada S, Noda T, Takahashi T, Hirokawa N (1995)
838 Synapsin I deficiency results in the structural change in the presynaptic terminals in the murine
839 nervous system. J Cell Biol 131:1789–1800.

840 Terada S, Tsujimoto T, Takei Y, Takahashi T, Hirokawa N (1999) Impairment of inhibitory synaptic
841 transmission in mice lacking synapsin I. J Cell Biol 145:1039–1048.

842 Torborg CL, Nakashiba T, Tonegawa S, McBain CJ (2010) Control of CA3 Output by Feedforward
843 Inhibition Despite Developmental Changes in the Excitation–Inhibition Balance. J Neurosci
844 30:15628–15637.

845 Toth K, Suares G, Lawrence JJ, Philips-Tansey E, McBain CJ (2000) Differential mechanisms of
846 transmission at three types of mossy fiber synapse. J Neurosci 20:8279–8289.

847 Valente P, Casagrande S, Nieus T, Verstegen AMJ, Valtorta F, Benfenati F, Baldelli P (2012) Site-
848 specific synapsin I phosphorylation participates in the expression of post-tetanic potentiation and its
849 enhancement by BDNF. J Neurosci 32:5868–5879.

850 Vandael D, Borges-Merjane C, Zhang X, Jonas P (2020) Short-Term Plasticity at Hippocampal Mossy
851 Fiber Synapses Is Induced by Natural Activity Patterns and Associated with Vesicle Pool Engram
852 Formation. Neuron 107:509-521.e7.

853 Vasileva M, Horstmann H, Geumann C, Gitler D, Kuner T (2012) Synapsin-dependent reserve pool of
854 synaptic vesicles supports replenishment of the readily releasable pool under intense synaptic
855 transmission. Eur J Neurosci 36:3005–3020.

856 Vyleta NP, Borges-Merjane C, Jonas P (2016) Plasticity-dependent, full detonation at hippocampal
857 mossy fiber-CA3 pyramidal neuron synapses. Elife 5:1–12.

858 Weisskopf MG, Castillo PE, Zalutsky RA, Nicoll RA (1994) Mediation of hippocampal mossy fiber
859 long-term potentiation by cyclic AMP. Science 265:1878–1882.

860 Wesseling JF, Lo DC (2002) Limit on the role of activity in controlling the release-ready supply of
861 synaptic vesicles. J Neurosci 22:9708–9720.

862 Zalutsky RA, Nicoll RA (1990) Comparison of two forms of long-term potentiation in single
863 hippocampal neurons. Science 248:1619–1624.

864 Zhang M, Augustine GJ (2021) Synapsins and the synaptic vesicle reserve pool: Floats or anchors?
865 Cells 10:1–13.

866 Zucker RS, Regehr WG (2002) Short-Term Synaptic Plasticity. Annu Rev Physiol 64:355–405.

867 Tables and figures

868 ***Table 1: SAGER guidelines checklist – other studies (applied sciences, cell biology, etc.).*** *Adapted from* Heidari et al., 2016.
869 **These points extend beyond the original SAGER table.*

Section/ Topic	**Item number**	**Checklist item**	**Reported on page number**
General	1	The terms sex/gender used appropriately	
Title	2a	Title specifies the sex of animals or any cells, tissues, and other material derived from these	1
	2b	In applied sciences (technology, engineering, etc.), the title indicates if the study model was based on one sex/gender or the application was considered for the use of one specific sex/gender	
Abstract	3a	Abstract specifies sex of animals or any cells, tissues, and other material derived from these	4
	3b	In applied sciences (technology, engineering, etc.), the abstract indicates if the study model was based on one sex/gender or the application was considered for the use of one specific sex/gender	
Introduction	4a	If relevant, previous studies that show presence or lack of sex or gender differences or similarities are cited	

	4b	Mention of whether sex/gender might be an important variant and if differences might be expected	
Methods	5a	In cell biological, molecular biological, or biochemical experiments, the origin and sex chromosome constitutions of cells or tissue cultures are stated. If unknown, the reasons are stated	
	5b	For studies testing devices or technology, explanation of whether the product will be applied or used by all genders and if it has been tested with a user's gender in mind	
	5c	If relevant, description of how sex/gender was considered in the design	
	5d	For in-vivo and in-vitro studies using primary cultures of cells, or cell lines from humans or animals, or ex-vivo studies with tissues from humans or animals, the sex of the subjects or source donors is stated (except for immortalized cell lines, which are highly transformed)	7
Results	6	For studies using animal models, present a sex breakdown of the animals*	
Discussion	7	If relevant, potential implications of sex/gender on the study results and analyses, including the extent to which the findings can be generalized to all sexes/genders in a population	26

870

871

872 ***Table 2: The ARRIVE guidelines 2.0 checklist: the essential ten.*** *Adapted from* Percie du Sert et al., 2020.

Item	**Item number**	**Recommendation**	**Reported in section**
Study design	1	For each experiment, provide brief details of study design including:	
	a.	The groups being compared, including control groups. If no control group has been used, the rationale should be stated.	Methods, study design & Results
	b.	The experimental unit (e.g. a single animal, litter, or cage of animals).	Methods, table 5 & Study design
Sample size	2 a.	Specify the exact number of experimental units allocated to each group, and the total number in each experiment. Also indicate the total number of animals used.	Methods, table 5 & Study design
	b.	Explain how the sample size was decided. Provide details of any *a priori* sample size calculation, if done.	Methods, Study design
Inclusion and exclusion criteria	3 a.	Describe any criteria used for including and excluding animals (or experimental units) during the experiment, and data points during the analysis. Specify if these criteria were established *a priori*. If no criteria were set, state this explicitly.	Methods, Field recordings
	b.	For each experimental group, report any animals, experimental units or data points not included in the analysis and explain why. If there were no exclusions, state so.	Methods, table 5 and table 6

		c.	For each analysis, report the exact value of n in each experimental group.	Methods, table 5 and study design
Randomi-sation	4	a.	State whether randomization was used to allocate experimental units to control and treatment groups. If done, provide the method used to generate the randomization sequence.	Methods, study design
		b.	Describe the strategy used to minimize potential confounders such as the order of treatments and measurements, or animal/cage location. If confounders were not controlled, state this explicitly.	Methods, study design
Blinding	5		Describe who was aware of the group allocation at the different stages of the experiment (during the allocation, the conduct of the experiment, the outcome assessment, and the data analysis).	Methods, study design
Outcome measures	6	a.	Clearly define all outcome measures assessed (e.g. cell death, molecular markers, or behavioral changes).	Results; Methods, table 5 and TEM analysis sections
		b.	For hypothesis-testing studies, specify the primary outcome measure, i.e. the outcome measure that was used to determine the sample size.	
Statistical methods	7	a.	Provide details of the statistical methods used for each analysis, including software used.	Methods, statistics
		b.	Describe any methods used to assess whether the data met the assumptions of the statistical approach, and what was done if the assumptions were not met.	Methods, statistics

Experimental animals	8	a.	Provide species-appropriate details of the animals used, including species, strain and substrain, sex, age or developmental stage, and, if relevant, weight.	Methods, study design & key resources table
		b.	Provide further relevant information on the provenance of animals, health/immune status, genetic modification status, genotype, and any previous procedures.	Methods, study design; Results; Discussion
Experimental procedures	9		For each experimental group, including controls, describe the procedures in enough detail to allow others to replicate them, including:	
		a.	What was done, how it was done and what was used.	Methods
		b.	When and how often.	Methods, table 5 and TEM
		c.	Where (including detail of any acclimatization periods).	Methods, Acute slice preparation, field recording and TEM
		d.	Why (provide rationale for procedures).	Introduction; Results; Discussion; Methods
Results	10		For each experiment conducted, including independent replications, report:	
		a.	Summary/descriptive statistics for each experimental group, with a measure of variability where	Results, text and figure legends

		applicable (e.g. mean and SD, or median and range).	
	b.	If applicable, the effect size with a confidence interval.	

873

874 ***Table 3: The ARRIVE guidelines 2.0: the recommended set.*** *Adapted from* Percie du Sert et al., 2020.

Item	**Item number**	**Recommendation**	**Reported in section**
Abstract	11	Provide an accurate summary of the research objectives, animal species, strain and sex, key methods, principal findings, and study conclusions.	Abstract
Background	12 a.	Include sufficient scientific background to understand the rationale and context for the study, and explain the experimental approach.	Introduction; Results; Discussion
	b.	Explain how the animal species and model used address the scientific objectives and, where appropriate, the relevance to human biology.	Introduction; Results; Discussion
Objectives	13	Clearly describe the research question, research objectives and, where appropriate, specific hypotheses being tested.	Abstract; Introduction; Results; Discussion
Ethical statement	14	Provide the name of the ethical review committee or equivalent that has approved the use of animals in this study, and any relevant license or protocol numbers (if applicable). If ethical approval was not sought or granted, provide a justification.	Methods, ethics statement
Housing and husbandry	15	Provide details of housing and husbandry conditions, including any environmental enrichment.	Methods, Acute slice preparation
Animal care and monitoring	16 a.	Describe any interventions or steps taken in the experimental protocols to reduce pain, suffering and distress.	Methods, Acute slice preparation
	b.	Report any expected or unexpected adverse events.	

		c.	Describe the humane endpoints established for the study, the signs that were monitored and the frequency of monitoring. If the study did not have humane endpoints, state this.	
Interpretation / scientific implications	17	a.	Interpret the results, taking into account the study objectives and hypotheses, current theory and other relevant studies in the literature.	Discussion
		b.	Comment on the study limitations including potential sources of bias, limitations of the animal model, and imprecision associated with the results.	Discussion, paragraph 9
Generaliza-bility/ translation	18		Comment on whether, and how, the findings of this study are likely to generalize to other species or experimental conditions, including any relevance to human biology (where appropriate).	Discussion, paragraph 9
Protocol registration	19		Provide a statement indicating whether a protocol (including the research question, key design features, and analysis plan) was prepared before the study, and if and where this protocol was registered.	
Data access	20		Provide a statement describing if and where study data are available.	Data availability statement
Declaration of interests	21	a.	Declare any potential conflicts of interest, including financial and non-financial. If none exist, this should be stated.	Conflict of interest statement
		b.	List all funding sources (including grant identifier) and the role of the funder(s) in the design, analysis and reporting of the study.	Acknowledgements

875

876 *Table 4: Statistical comparison for experimental values between two cohorts of presymptomatic SynTKO animals.*

Experiment	Measure	Presynaptic SynTKO animals from Italy	Presynaptic SynTKO animals from Berlin
Input-Output	Slope of simple linear regression	1.341	0.833
	Ranges of 95% confidence band	0.5494 to 2.134	0.09287 to 1.573
	p-value slopes (ANCOVA)	0.69	
1 Hz facilitation	Median	4.440	5.955
	Interquartile range	3.760 - 6.260	3.753 - 11.41
	p value (Mann-Whitney *U* test)	0.3473	
Paired-pulse ratio	Median	3.557	4.545
	Interquartile ranges	2.299 - 4.260	2.568 - 6.035
	p-value (Mann-Whitney *U* test)	0.0899	
PTP (norm. fEPSP)	Median	3.469	4.116
	Interquartile ranges	2.118 - 4.589	3.374 - 7.144
	p-value (Mann-Whitney *U* test)	0.1151	
LTP after 30 min (norm. fEPSP)	Median	245.2	228.8
	Interquartile ranges	198.3 - 302.9	182.5 - 384.4
	p-value (Mann-Whitney *U* test)	0.8793	

877

878 ***Table 5: Overview of slice and animal numbers for different experimental groups for field recordings.*** *Note: all numbers*

879 *reported for individual experiments are only from the included subset of recordings.*

s = number of slices a = number of animals	**C57BL/6J (4-6 weeks)**	**Synapsin TKO (4-6 weeks)**		**C57BL/6J (17-19 weeks)**	**Synapsin TKO (18 -19 weeks)**
		From Italy (4-5 weeks)	**From Berlin (4-6 weeks)**		
Recorded	s = 58 a = 10	s = 39 a = 9	s = 18 a = 7	s = 29 a = 5	s = 24 a = 5
Included	s = 26 a = 10	s = 24 a = 9	s = 14 a = 4	s = 17 a = 4	s = 19 a = 5
Input-Output Ratio	s = 26 a = 10	s = 23 a = 9	s = 14 a = 4	s = 17 a = 4	s = 18 a = 5
Paired-Pulse Ratio	s = 26 a = 10	s = 20 a = 8	s = 14 a = 4	s = 17 a = 4	s = 19 a = 5
1 Hz Facilitation	s = 26 a = 10	s = 15 a = 5	s = 12 a = 4	s = 17 a = 4	s = 19 a = 5
25 Hz Stimulation	s = 7 a = 3	s = 4 a = 3	s = 8 a = 3		
PTP + LTP	s = 11 a = 4	s = 13 a = 6	s = 10 a = 3		

880

881 ***Table 6: Exclusion reasons for field recordings.*** *Note that several reasons can apply to the same recording.*

Excluded recordings	**C57BL/6J (4-6 weeks)**	**Synapsin TKO (4-6 weeks)**	**C57BL/6J (17-19 weeks)**	**Synapsin TKO (18 -19 weeks)**
Total number	32	19	12	5
Baseline EPSP < 50 µV	4	2	2	2
DCG-IV effect < 75%	25	14	11	4
Other reasons	4	2	0	1

882

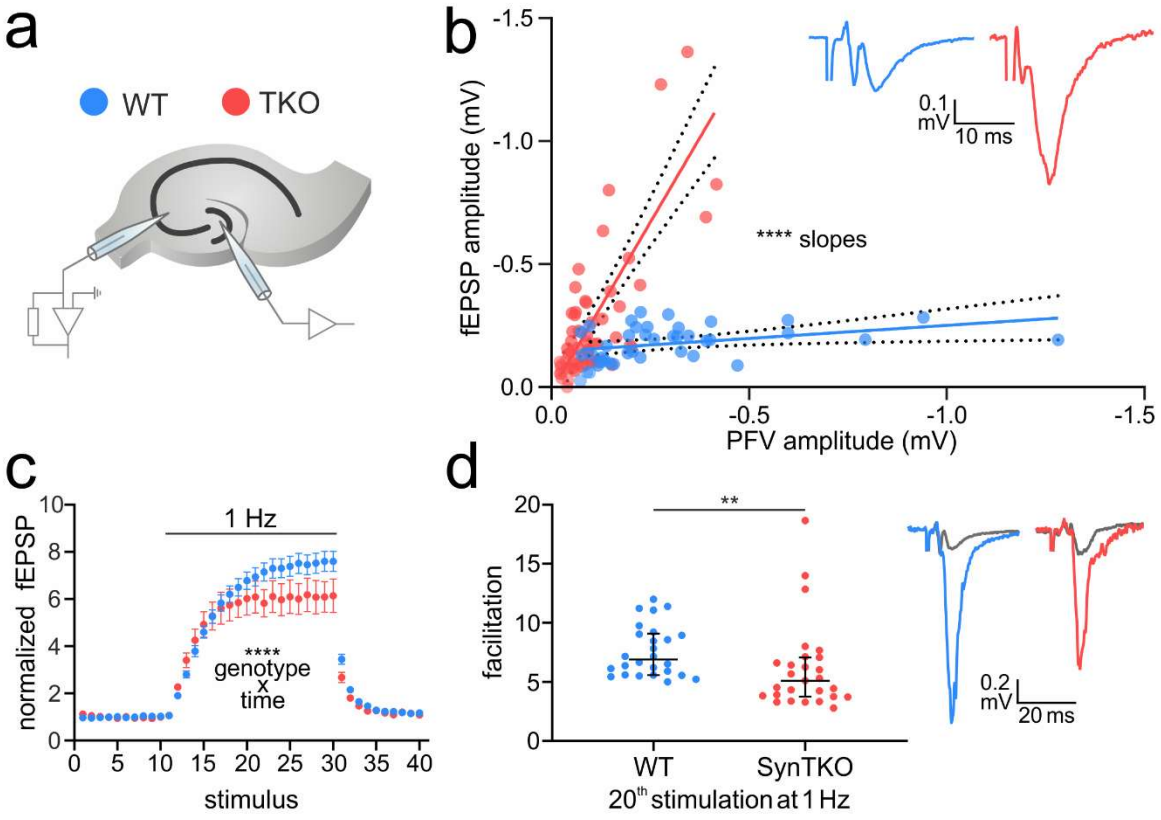

Figure 1: Increased excitability, but reduced facilitation, at mossy fibers of presymptomatic SynTKO mice. ***a)*** *Field recording setup for an acute brain slice. The stimulation electrode was placed in the hilus close to the granule cell layer of the dentate gyrus, the recording electrode was placed in the* stratum lucidum *of area CA3 of the hippocampus where mossy fibers terminate.* ***b)*** *Excitability was increased in brain slices from SynTKO mice (red; 37 slices from 13 animals) compared to WT mice (blue; 26 slices from 10 animals). Pooled fEPSP amplitudes (mV) were plotted against pooled presynaptic fiber volley (PFV) amplitudes (mV) and fitted with a simple linear regression. The slopes of the linear regressions were significantly different ($p < 0.0001$, tested with a two-tailed ANCOVA). 95% confident bands are shown as dotted lines around the fit.* ***Inset:*** *Example traces from WT (blue) and SynTKO (red) slices with similar PFV amplitudes. Note the difference in the corresponding fEPSP amplitude.* ***c)*** *Frequency facilitation is reduced in SynTKO (red) compared to WT (blue) slices. Averaged normalized fEPSP amplitudes +/- SEM from all WT (blue; 26 slices from 10 animals) and SynTKO (red; 27 slices from 9 animals) recordings plotted against the number of stimuli. Stimuli 1-10 were given with a frequency of 0.05 Hz, stimuli 11-30 with 1 Hz and stimuli 31-41 with a frequency of 0.05 Hz again. Both time and the interaction between genotype and time were significantly different in a mixed-effects model ($p < 0.0001$). Post-hoc Sidak's test for multiple comparisons revealed no significant differences.* ***d)*** *Facilitation was reduced in SynTKO compared to WT animals after 1 Hz frequency stimulation.* ***Left:*** *fEPSP amplitudes at the 20th stimulus at 1 Hz for individual WT (blue dots; 26 slices from 10 animals) and SynTKO (red dots; 27 slices from 9 animals) recordings. Median values +/- interquartile ranges are shown in black. Facilitation was significantly different ($p = 0.0029$, Mann-Whitney* U *test).* ***Right:*** *Example fEPSP amplitudes from WT (blue) and SynTKO (red) recordings at the 20th 1 Hz stimulus. Respective baseline fEPSP amplitudes are shown in grey.*

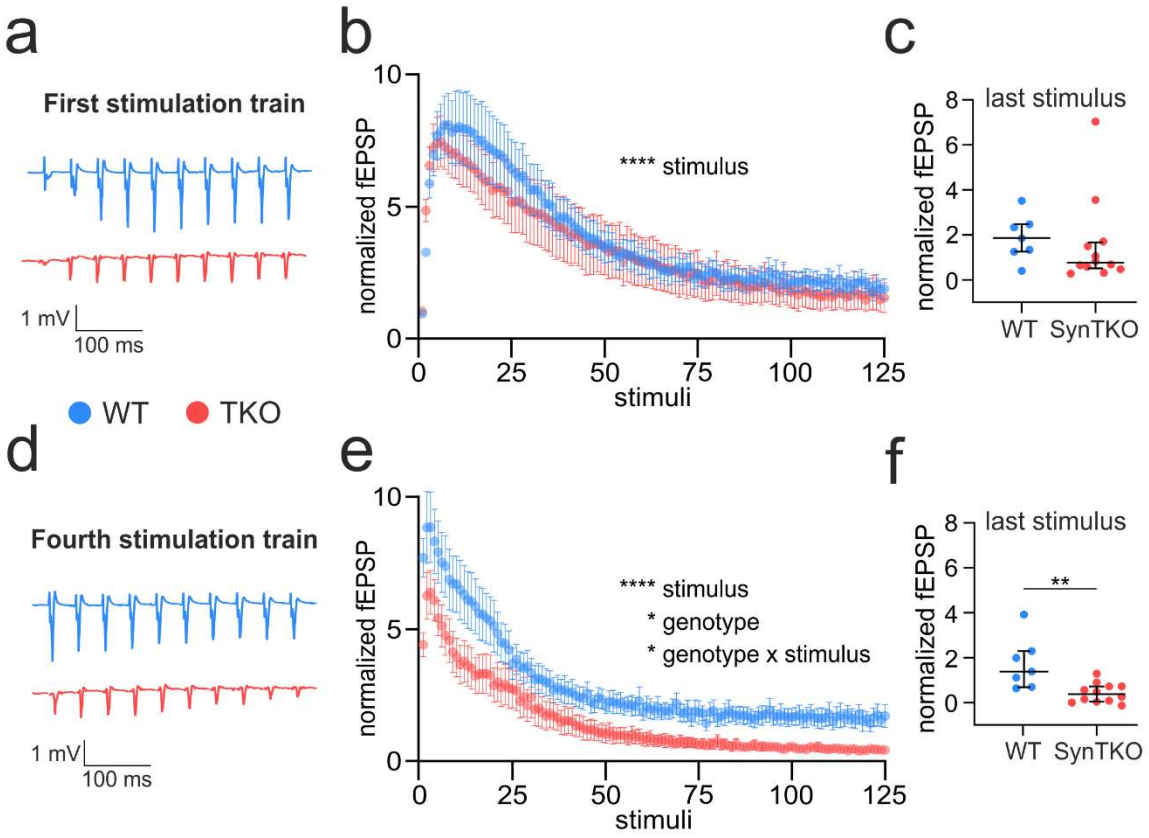

Figure 2: Faster depression during high-frequency stimulation in SynTKO mice. *High-frequency stimulation comprised four trains of 125 pulses at 25 Hz with an interval of 20 seconds between the first stimuli of consecutive trains.* ***a)*** *Example traces show fEPSP amplitudes of mossy fibers from WT (blue) and SynTKO (red) slices in response to the first 10 stimuli of the first high-frequency stimulation train.* ***b)*** *Normalized averaged fEPSP amplitudes plotted against number of stimuli of the first high-frequency stimulation train for WT (blue; 7 slices from 3 animals) and SynTKO (red; 12 slices from 6 animals) recordings. A mixed-effects model revealed no significant difference between genotypes ($p = 0.74$), but significant differences ($p < 0.0001$) for the factor time (stimulus). A post-hoc Sidak's test for multiple comparisons revealed no significant differences for single time points.* ***c)*** *Normalized fEPSP amplitudes at the last stimulus of the first stimulation train for individual WT (blue dots; 7 slices from 3 animals) and SynTKO (red dots; 12 slices from 6 animals) recordings. Median values +/- interquartile ranges are shown in black. Ranks were not significantly different ($p = 0.1956$, Mann-Whitney U test).* ***d)*** *Example traces show fEPSP amplitudes of WT (blue) and SynTKO (red) animals in response to the first 10 stimuli of the fourth high-frequency stimulation train.* ***e)*** *Normalized averaged fEPSP amplitudes plotted against number of stimuli of the first high-frequency stimulation train for WT (blue; 7 slices from 3 animals) and SynTKO (red; 12 slices from 6 animals) animals. Both the factors time (stimulus), genotype and the interaction of both were significantly different in a mixed-effects model ($p < 0.0001$ for time, $p = 0.02$ for the genotype and $p = 0.04$ for the interaction of genotype and time). A post-hoc Sidak's test for multiple comparisons revealed no significant differences for single time points.* ***f)*** *Normalized fEPSP amplitudes at the last stimulus of the fourth stimulation train for individual WT (blue dots; 7 slices from 3 animals) and SynTKO (red dots; 12 slices from 6 animals) recordings. Median values +/- interquartile ranges are shown in black. Ranks were significantly different ($p = 0.004$, Mann-Whitney U test).*

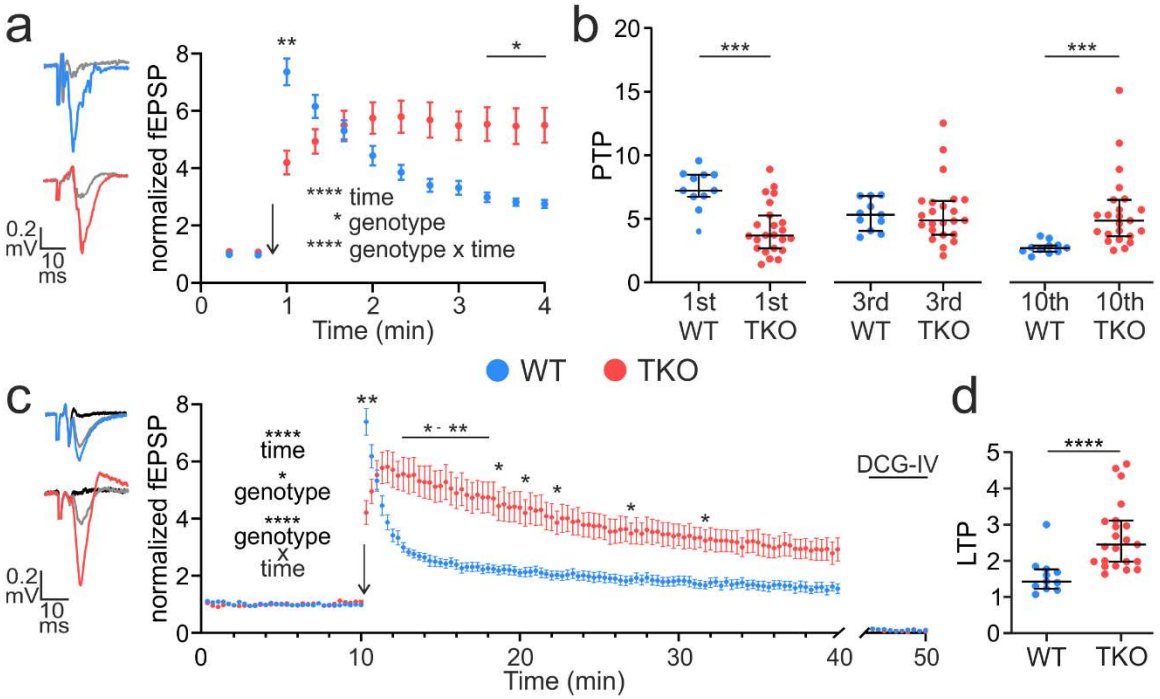

Figure 3: SynTKO mossy fibers display reduced post-tetanic potentiation but increased long-term potentiation. ***a)*** *Post-tetanic potentiation is decreased in SynTKO mossy fibers.* ***Left:*** *Example traces of the fEPSP amplitude at the first stimulus after high-frequency stimulation for mossy fibers from WT (blue, top) and TKO (red, bottom) mice compared to averaged baseline fEPSP amplitude (grey).* ***Right:*** *Normalized averaged fEPSP amplitudes plotted against time (min) from WT (blue; 11 slices from 4 animals) and SynTKO (red; 23 slices from 9 animals) recordings. This plot is a partial zoom-in from the plot shown in c (minutes 9-13). Mean values +/- SEM are shown. The arrow indicates the time point of high-frequency stimulation (4x 125 pulses @ 25 Hz). Stimulation before and after was at 0.05 Hz. Statistics for data set as reported in c.* ***b)*** *Scatter plots for individual fEPSP amplitudes for WT (blue) and SynTKO (red) recordings for the first, third and tenth stimulus after high-frequency stimulation, respectively. Median values +/- interquartile ranges are shown in black. Significance was tested with a Kruskal-Wallis test and a post-hoc Dunn's correction for multiple comparisons. The Kruskal-Wallis test revealed significant differences between ranks with $p < 0.0001$. Multiple comparisons revealed significant differences for the first ($p = 0.0002$) and tenth ($p = 0.001$) time point.* ***c)*** *LTP is increased in SynTKO animals after 30 min.* ***Left:*** *Example traces of fEPSP amplitudes 30 min after high-frequency stimulation for mossy fibers from WT (blue, top) and TKO (red, bottom) mice compared to baseline fEPSP amplitude (grey) and response to 1 µM DCG-IV (black).* ***Right:*** *Normalized averaged fEPSP amplitudes plotted over time (min) from WT (blue; 11 slices from 4 animals) and SynTKO (red; 23 slices from 9 animals) recordings. Mean values +/- SEM are shown. The arrow indicates the high-frequency stimulation (4x 125 pulses @ 25 Hz). Stimulation frequency before (baseline) and after (LTP recording) was 0.05 Hz. At the end of the recording, 1 µM DCG-IV was washed in to ensure mossy fiber specificity. The last ten fEPSP amplitudes during DCG-IV wash-in are shown at the end of the recording. A mixed-effects model revealed significant differences for the genotype ($p = 0.01$), time ($p < 0.0001$) and the interaction of both ($p < 0.0001$). A post-hoc Sidak's test for multiple comparisons revealed significant differences for the first sweep after high-frequency stimulation ($p = 0.005$) and sweeps 38-54 (p: 0.009 – 0.05; ~13-18 min), as well as for sweeps 56, 61, 67, 81*

944 *and 94 (p: 0.03 - 0.04; ~ minutes 19, 20, 22, 27 and 32).* ***d)*** *Dots indicate averaged fEPSP amplitudes from individual WT*

945 *(blue) and SynTKO (red) recordings. Amplitudes were averaged over the last 10 minutes of the LTP recording; from 20 – 30*

946 *min after high-frequency stimulation. Median values +/- interquartile ranges are shown in black. Ranks were significantly*

947 *different with* $p < 0.0001$ *(Mann-Whitney* U *test).*

948

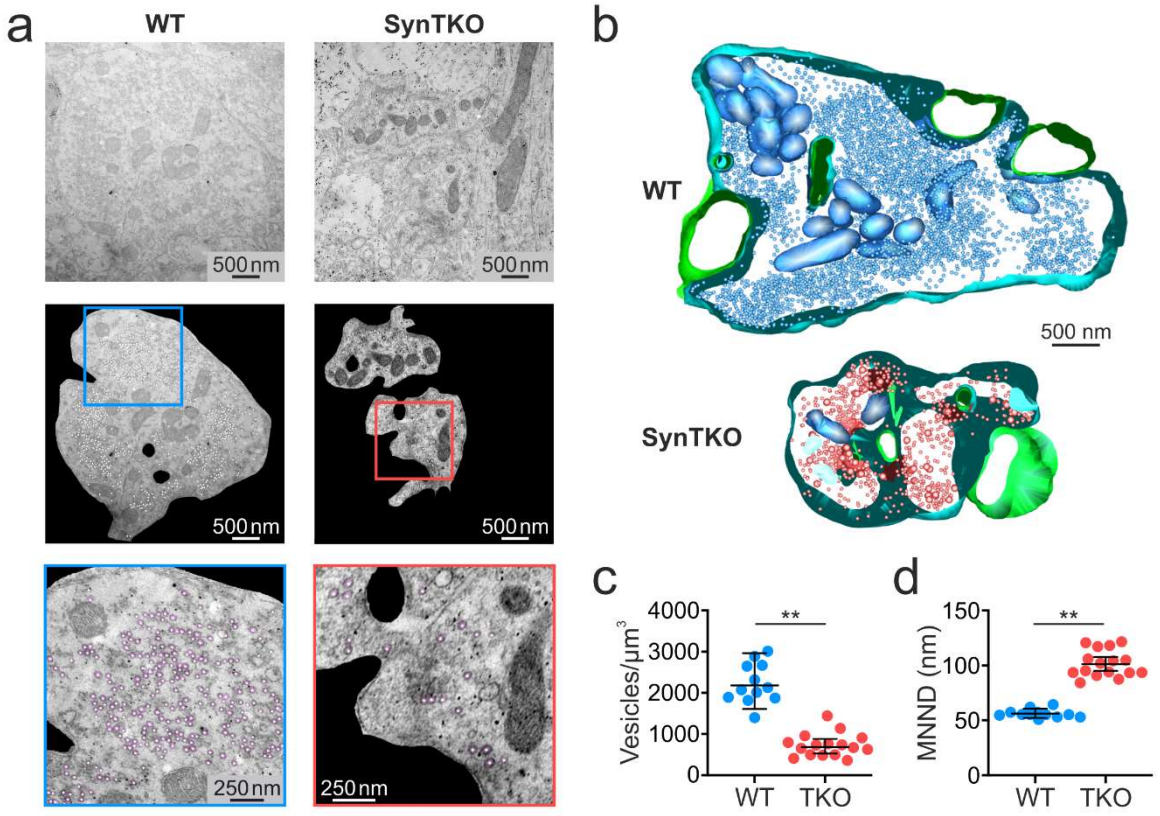

Figure 4: Synaptic vesicles are more dispersed in mossy fiber* boutons *from SynTKO mice. ***a)*** *In mossy fiber* boutons *synaptic vesicles are more dispersed and their density is reduced. Example images from transmission electron microscopy (TEM) showing mossy fiber boutons from WT (left) and SynTKO (right) animals.* ***Top:*** *Raw TEM images of mossy fiber* boutons *in* stratum lucidum*.* ***Middle:*** *An automated tool (Imbrosci et al., 2022) was used to detect vesicles. Mossy fiber* boutons *were extracted from the raw image and the center of detected vesicles is marked with a white dot. Blue and red boxes show the region for the zoom-ins in WT and SynTKO, respectively.* ***Bottom:*** *Zoom-ins, as marked in the middle pictures. Vesicles detected by the algorithm are shown in purple.* ***b)*** *Partial 3D reconstruction of hippocampal mossy fiber* boutons *from a WT (top) and a SynTKO animal (bottom) for visualization purposes only. Vesicles are shown in blue and red respectively, the presynaptic mossy fiber membrane is shown in light blue and postsynaptic spines are shown in green.* ***c)*** *The number of synaptic vesicles per µm³ is reduced in SynTKO animals. Dots represent the number of vesicles in individual mossy fiber* boutons *from 2 WT (blue; 12* boutons*) and 3 SynTKO (red; 16* boutons*) animals. Mean values and the borders of the 95% confidence intervals are shown in black. A generalized linear mixed model (gamma family with log link) revealed significant differences between genotypes with p = 0.006.* ***d)*** *The mean nearest neighbor distance (MNND) is increased between synaptic vesicles in SynTKO compared to WT* boutons*. Scatter plot shows average MNND (nm) for individual mossy fiber* boutons *from 2 WT (blue; 12* boutons*) and 3 SynTKO (red; 16* boutons*) animals. Genotypes were significantly different in a generalized linear mixed model (gamma family with log link) with p = 0.0015. Mean values are shown in black with the borders of the 95% confidence intervals.*

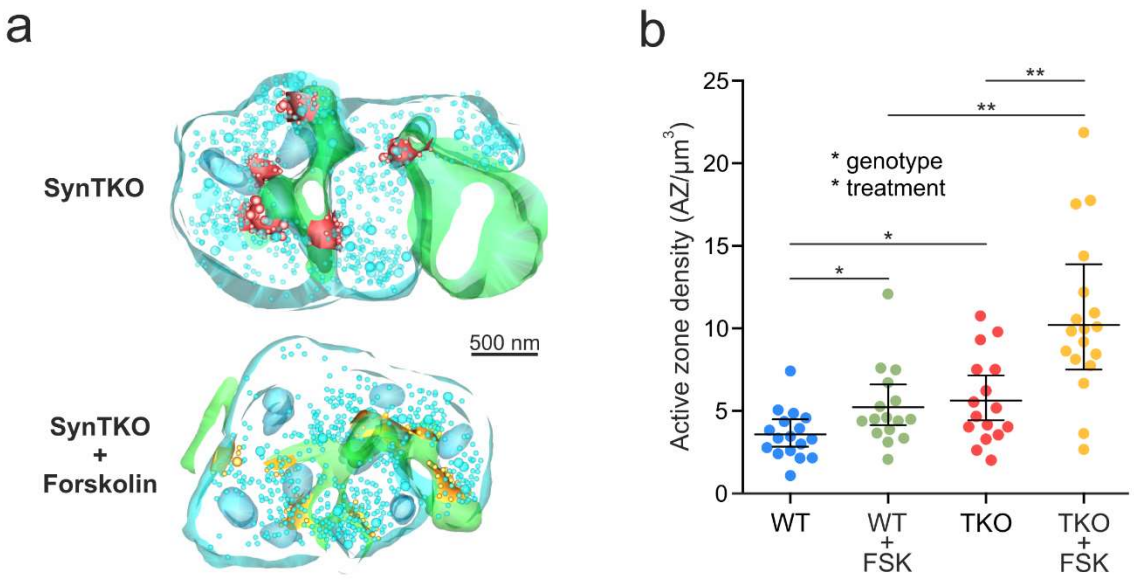

Figure 5*: *Increased active zone density in mossy fiber* boutons *of SynTKO mice. ***a)*** *Example partial 3D reconstructions of mossy fiber* boutons *from untreated (top) and forskolin-treated (bottom) SynTKO mice. Active zones with docked vesicles are shown in red (SynTKO) and yellow (SynTKO + forskolin), respectively. Synaptic vesicles, mitochondria and presynaptic membrane are shown in light blue, postsynaptic membrane is shown in green.* ***b)*** *Number of active zones per µm³ plotted for individual mossy fiber* boutons *from untreated WT (blue dots; 17* boutons *from 3 animals) and untreated SynTKO slices (red dots; 16* boutons *from 3 animals) as well as for forskolin-treated WT (green dots; 16* boutons *from 3 animals) and forskolin-treated SynTKO slices (yellow dots; 18* boutons *from 3 animals). Mean values are shown in black with upper and lower borders of the 95% confidence interval. A generalized linear mixed model (gamma family with log link) revealed significant differences for genotype (p = 0.01) and forskolin treatment (p = 0.013). A post-hoc test (estimated marginal means with false discovery rate correction) revealed significant differences between WT and SynTKO (p = 0.0125), WT and WT + forskolin (p = 0.0134), SynTKO and SynTKO + forskolin (p = 0.0018) and WT + forskolin and SynTKO + forskolin (p = 0.0018), but no significant difference between WT + forskolin and SynTKO (p = 0.658).*

Supplementary figures

Figure 1-1: Increased excitability, but reduced facilitation, at mossy fibers of symptomatic SynTKO. ***a)*** *Field recording setup for an acute brain slice. The stimulation electrode was placed in the hilus close to the granule cell layer of the dentate gyrus, the recording electrode was placed in the* stratum lucidum *of area CA3 of the hippocampus where mossy fibers terminate.* ***b)*** *Excitability was increased in recordings from SynTKO mice (red; 18 slices from 5 animals) compared to WT mice (blue; 17 slices from 4 animals). Pooled fEPSP amplitudes (mV) were plotted against pooled presynaptic fiber volley (PFV) amplitudes (mV) and fitted with a simple linear regression. The slopes of the linear regressions were significantly different ($p < 0.0001$, tested with a two-tailed ANCOVA). 95% confidence bands are shown as dotted lines around the fit.* ***Inset:*** *Example traces from WT (blue) and SynTKO (red) animals with similar PFV amplitudes. Note the difference in the corresponding fEPSP amplitude.* ***c)*** *Frequency facilitation was reduced in SynTKO (red) compared to WT (blue) animals. Averaged normalized fEPSP amplitudes +/- SEM from all WT (blue; 17 slices from 4 animals) and SynTKO (red; 19 slices from 5 animals) recordings plotted against the number of stimuli. Stimuli 1-10 were given with a frequency of 0.05 Hz, stimuli 11-30 with 1 Hz and stimuli 31-41 with a frequency of 0.05 Hz again. Both time and the interaction between genotype and time were significantly different in a mixed-effects model ($p < 0.0001$). Post-hoc Sidak's test for multiple comparisons revealed significant differences ($p < 0.05$) for two time points (indicated with *).* ***d)*** *Facilitation was reduced in SynTKO compared to WT animals after moderate frequency stimulation.* ***Left:*** *fEPSP amplitudes at the 20th stimulus at 1 Hz for individual WT (blue dots; 17 slices from 4 animals) and SynTKO (red dots; 19 slices from 5 animals) recordings. Median values +/- interquartile ranges are shown in black. Facilitation was significantly different ($p = 0.0009$, tested with Mann-Whitney* U *test).* ***Right:*** *Example fEPSP amplitudes from WT (blue) and SynTKO (red) animals at the 20th 1 Hz stimulus. Respective baseline fEPSP amplitudes are shown in grey.*

Figure 1-2: Paired-pulse ratio not significantly changed in presymptomatic SynTKO mice. a) *Paired-pulse ratio for presymptomatic SynTKO and age-matched control animals.* ***Top:*** *Example traces for a paired-pulse from WT (blue) and SynTKO (red) recordings, respectively.* ***Bottom:*** *Dots represent paired-pulse ratios from individual recordings from WT (blue dots, 26 slices from 10 animals) and SynTKO (red dots, 34 slices from 12 animals) slices, calculated as the ratio of second to first fEPSP amplitude. The inter-stimulus interval (ISI) was 50 ms. Median values +/- interquartile ranges are depicted in black. Ranks were compared in a Mann-Whitney* U *test and were not significantly different (p = 0.226).* ***b)*** *Paired-pulse ratio for presymptomatic SynTKO (red) animals and age-matched controls (blue) with a shorter ISI. Dots represent individual paired-pulse ratio of the first two stimuli from the 25 Hz stimulation train (Figure 2a,b) with an ISI of 40 ms, for WT (blue dots, 7 slices from 3 animals) and SynTKO (red dots, 12 slices from 6 animals) recordings. Median values +/- interquartile ranges are depicted in black. Ranks were tested with a Mann-Whitney* U *test and were not significantly different (p = 0.142).* ***c)*** *Paired-pulse ratio for symptomatic SynTKO and age-matched control animals.* ***Top:*** *Example traces for a paired-pulse from WT (dark blue) and SynTKO (dark red) recordings, respectively.* ***Bottom:*** *Dots represent paired-pulse ratios from individual recordings from WT (dark blue dots, 17 slices from 4 animals) and SynTKO (dark red dots, 19 slices from 5 animals) slices, calculated as the ratio of second to first fEPSP amplitude. The inter-stimulus interval (ISI) was 50 ms. Median values +/- interquartile ranges are depicted in black. Ranks were compared in a Mann-Whitney* U *test and were significantly different (p = 0.0325).*

Figure 2-1: The loss of fibers during high-frequency stimulation is not substantial and similar for SynTKO and WT mice. ***a)*** *Exemplary traces from high-frequency stimulation trains for WT (blue) and SynTKO (red) animals. The 10th PFV and fEPSP from the first and fourth stimulation train are depicted, respectively. Dotted lines indicate the peaks of the PFV. Note that although the PFV is smaller for SynTKO (due to technical reasons in response to the high excitability), the size is relatively consistent throughout the trains.* ***b)*** *Averaged PFV (mV) taken from pulses 10-15 from the first and fourth stimulation train, respectively, for recordings from WT (blue; 7 slices from 3 animals) and SynTKO (red; 12 slices from 6 animals) slices. Average values from the same recording are connected. Median values +/- interquartile ranges are depicted in black. Ranks between first and fourth stimulation train were not significantly different for neither WT ($p = 0.16$) nor SynTKO ($p = 0.08$) recordings, compared with a Wilcoxon test.* ***c)*** *The relative loss of fibers was similar for WT and SynTKO recordings. Averaged ratios between 4th and 1st train PFV sizes are depicted for both WT (blue; 7 slices from 3 animals) and SynTKO (red; 12 slices from 6 animals) animals. Median values +/- interquartile ranges are depicted in black. Ranks were not significantly different ($p = 0.45$) in a Mann-Whitney* U *test.*